

# Chapter 7: Neuronavigation

Stefan M. Goetz, PhD<sup>1</sup>

Thomas Kammer, MD<sup>2</sup>

## Abstract

The relatively high focality of transcranial brain stimulation requires accurate targeting of the fields delivered to the brain in order to stimulate the neural circuits that mediate the intended effect while reducing the unintended exposure of other brain areas. A range of tools support accurate individualized targeting of transcranial stimulation. Since targets are increasingly defined through anatomical, functional, or connectivity imaging, individualized gyrus-precise head models help to identify optimal placement of the stimulation transducers. Neuronavigation systems, such as frameless stereotaxy, can enable accurate delivery of stimulation to these targets. This is achieved by real-time tracking of the stimulation transducer and the subject's head, and co-registering the head position to a computer model of the head anatomy and other target information. Whereas neuronavigation is currently limited to the spatial positioning of the transducers relative to the brain target, stimulation technologies that introduce functional or neuron-type-specific selectivity will demand novel tools for optimal targeting. As real-time simulation and robot-assisted motion-compensated transducer placement become feasible, technology is trending towards the convergence of computational intervention planning and neuronavigation.

**Keywords:** Target identification; transsynaptic targeting; navigated neurostimulation; real-time physical modeling; robotic coil placement.

## Introduction

Brain stimulation technologies can leverage their spatial focality to exploit the anatomical organization of brain functions, especially in the cortex (see Section III of this book). Transcranial magnetic stimulation (TMS), for instance, offers stimulation coils that allow relatively selective stimulation of cortex volumes as small as approximately 5 mm × 5 mm × 5 mm (see Chapter 4), and the focality of transcranial electrical stimulation (tES) has been improved similarly (see Chapter 2) (Thielscher and Kammer 2004; Dmochowski et al. 2011; Groppa et al. 2012; Goetz and Deng 2017). Other stimulation and modulation technologies, such as transcranial (focused continuous or pulsed) ultrasound (Chapter 9), further allow focusing in depth (Lee et al. 2016). However, the focality of stimulation methods requires accurate determination and maintenance of the stimulation transducer placement relative to the brain target.

Such accurate targeting typically involves the selection of targeting parameters such that the stimulation effect in the target brain area is maximized. The placement of the stimulation transducers is the key targeting parameter. In electrical stimulation, for instance, the shape, size, and position of the electrodes as well as the polarity of the individual electrode's current determine the spatial distribution of the electric field inside the brain (Rawji et al. 2018; Saturnino, Antunes, and

---

<sup>1</sup> University of Cambridge, CB2 1PZ, UK and Duke University, Durham, NC 27710, USA

<sup>2</sup> Universität Ulm, BW 89069, Germany

Thielscher 2015; Alam et al. 2016; Edwards et al. 2013; Bikson, Rahman, and Datta 2012). In TMS, the equivalent spatial degrees of freedom for the operator to influence the stimulation target are the position and orientation of the coil relative to the brain, as well as the current direction of the pulse (Kammer, Beck, Erb, et al. 2001; Thielscher and Kammer 2002; Brasil-Neto et al. 1992; Mills, Boniface, and Schubert 1992). In ultrasound stimulation, the main targeting parameters are the type, position, and orientation of the transducer, whereas the frequency is typically preselected (Tufail et al. 2010; Tufail et al. 2011; Lee et al. 2016; Wattiez et al. 2017). Ultrasound stimulation can be pulsed or quasi-continuous. Some advanced stimulation systems synthesize the field or wave front inside the head through the superposition of several transducers. Such multichannel targeting is technically most straightforward with electrical and ultrasound arrays, but early-stage technical solutions also exist for TMS (Dmochowski et al. 2011; Villamar et al. 2013; Bikson et al. 2014; Fischer et al. 2017; Clement and Hynynen 2002; Groppa et al. 2012; Koponen, Nieminen, and Ilmoniemi 2018; Ruohonen and Ilmoniemi 1998). Accordingly, the number of parameters for targeting increases as each channel affects the spatial field distribution. In such multichannel systems, the degrees of freedom, such as current amplitude or position, of the different transducers are often generated computationally.

In addition to the spatial targeting parameters, advanced devices introduce even more degrees of freedom related to the stimulus waveform in electrical and magnetic stimulation (see Chapter 5), which can provide some extent of activation selectivity at the neuron level (D'Ostilio et al. 2016; Goetz et al. 2016; Sommer et al. 2018; Halawa et al. 2019). To date, such features are not yet supported by any targeting or navigation toolbox.

Despite their similarities, the various stimulation technologies differ in several aspects relevant for targeting. In TMS, the spatial distribution of the induced electric field is largely determined by the coil, as the conductivity of brain tissues is relatively low. Nevertheless, the electric field is locally distorted by the individual head anatomy such as the cortical gyrification patterns as well as the large difference in conductivity between the corticospinal fluid and the brain (see Chapters 1 and 6). Accordingly, the location of the strongest stimulation can be assumed to be approximately underneath the area of the coil where the winding is densest and closest to the scalp. For example, stimulation is strongest underneath the center of a figure-of-eight coil. The exact location, however, can be markedly shifted due to the brain's gyrification (Opitz et al. 2011; Thielscher, Opitz, and Windhoff 2011; Bijsterbosch et al. 2012; Raffin et al. 2015). In contrast to magnetic stimulation, in electrical stimulation the current injected by the electrodes has to pass through the scalp, the skull including current-shunting openings such as the orbits, the cerebrospinal fluid, and other head tissues with diverse structure and electrical conductivities before reaching the brain, resulting in a complex flow pattern following the path of highest electrical conductivity (Datta et al. 2009). Moreover, the current can reach deep brain regions where it is shaped by the structure of the cortex, white matter, subcortical structures, and ventricles. Accordingly, the spatial distribution of the electric field is determined by the individual anatomy, and estimation of the stimulated target is not trivial for an operator. Similarly, ultrasound is strongly affected by the mechanical tissue properties, scattered, and partially reflected at material interfaces (Clement and Hynynen 2002; Pinton et al. 2012).

Importantly, the focality of some stimulation paradigms, such as TMS, has reached a level where further focality enhancement might be limited by the ability to reliably target smaller locations and maintaining this target throughout an extended period of time despite small head or skin movements during a stimulation session. Thus, even if higher spatial focality—ideally down to the single-neuron level—became available, better methods for targeting and fixing the transducers will become critical.

In addition to the technical problem of ensuring that stimulation is focused on specific brain targets, the selection of these targets can be challenging as well. The target selection is rarely based on an exactly known location but typically aims to modulate a specific brain function.

A number of technical means can support planning and execution of the targeting of a brain stimulation intervention. These include prediction of the stimulated brain areas through simulations based on the transducer placement and individual head anatomy scans, quantification and display of the position of transducers relative to the brain through neuronavigation, and holding or stabilizing transducers in mechanical arms or robots. Importantly, all these tools rely on many assumptions and, in some cases, may mislead users to believe there is an unrealistically high level of precision and accuracy. Therefore, operators should be experienced in how to reliably use the tools and to identify factors that degrade targeting performance. In addition, there should be a sustained effort by manufacturers and users to quantify and improve the overall accuracy and precision of neuronavigation tools.

### Role and elements of targeting

The goal of neuronavigation is to increase the specificity, strength, and reliability of brain stimulation effects. Taking TMS as an example, most applications use a focal coil, restricting the effective field strengths to a small volume of the brain situated close to the coil, typically in the neocortex. Nevertheless, some interventions, such as one depression treatment protocol, have achieved good results with relatively unfocused fields (Levkovitz et al. 2015; Deng, Lisanby, and Peterchev 2013). Thus, the intended effects are based on neurophysiological modulation of a specific part of the neocortex, reflecting spatial organization and separation of many brain functions (Van Essen et al. 1998). This extends to most other stimulation paradigms, some of which, such as ultrasound, allow for relatively selective targeting of deeper brain structures.

Targeting typically comprises several components. The first component refers to target identification, i.e., the specification of the neural structure to be stimulated or modulated and its precise location in the individual patient or subject. Various technologies can support this step by leveraging the brain's anatomy, neurophysiology, and connectivity. The second component involves the selection of the specific targeting parameters of the stimulation or modulation technology, typically by positioning the stimulation source, including location and orientation. Computational methods and models might in the future replace or supplement intuition and conventional transducer placement on the scalp directly over the target. The corresponding positioning of transducers can be performed manually by the operator with the support of a navigation system that reports any deviations, or by a robotic positioning system (Krings, Chiappa, et al. 2001; Lancaster et al. 2004). In multichannel stimulation systems, the stimulator can usually adjust the contribution of the various channels to shift the focus and direct it to the target. Furthermore, targeting should be maintainable and reproducible within and across stimulation sessions. Finally, targeting involves documentation of the stimulation site, both for reporting of the findings and for interventions where the location and related parameters are a major part of the outcome, such as mapping of brain function (motor cortex, e.g., Julkunen 2014; visual cortex, e.g., Kammer et al. 2005), which can be used for presurgical planning (Krings, Foltys, et al. 2001; Picht et al. 2011; Takahashi and Picht 2014; Weiss Lucas et al. 2020; Jeltema et al. 2021).

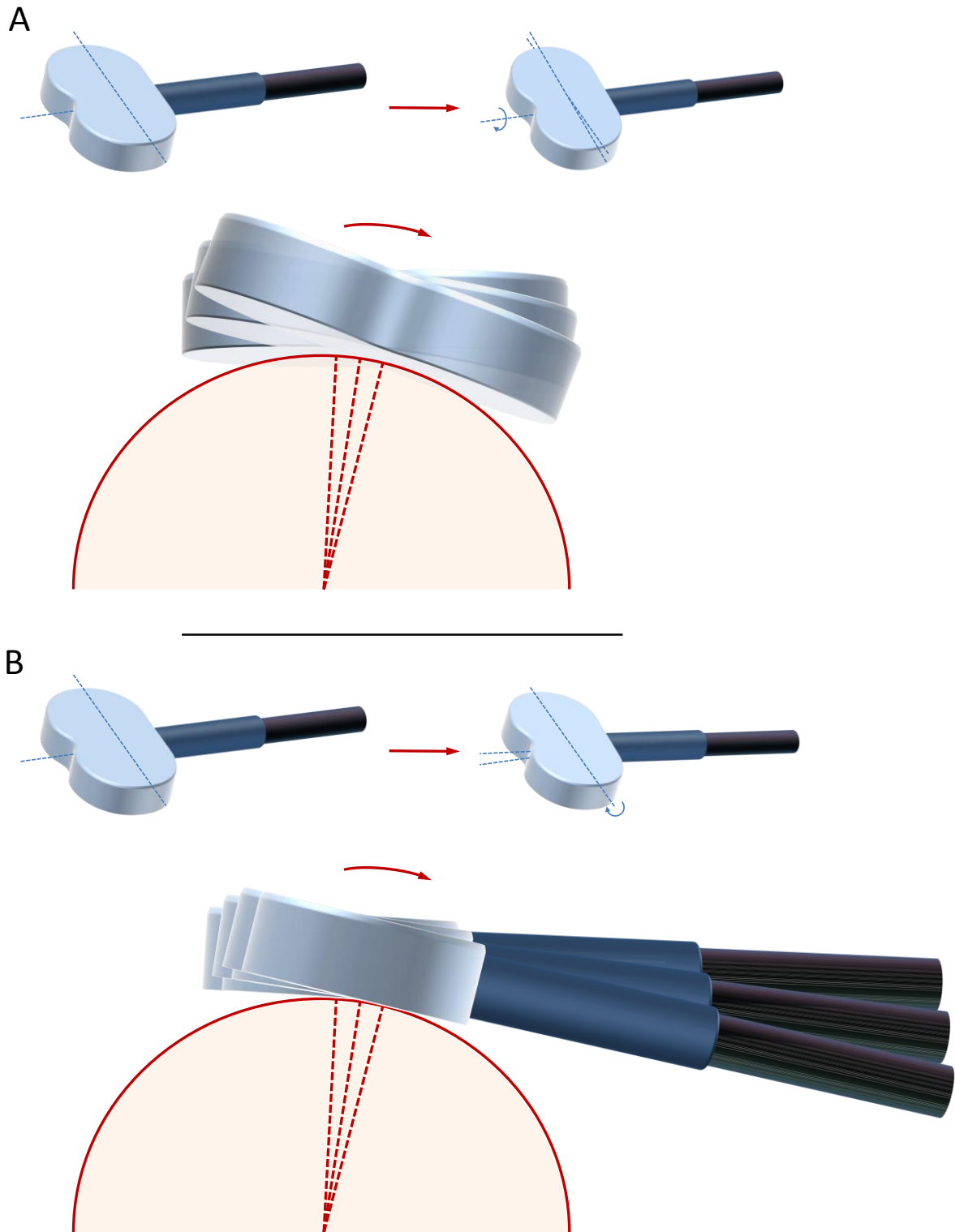


**Figure 7.1 about here**

**Caption:** Importance of transducer orientation: Even small deviations in the orientation lift the focus point of a TMS coil off the head and the coil touches the head at another part of the coil surface (often closer to the coil handle). A deviation of a few degrees can shift the stimulated location in the brain by millimeters. This problem is likewise important in focal ultrasound stimulation. For both, the orientation of the transducer plane relative to the local head normal is most important, which has two axes, shown in Panels A and B. For TMS, rotation around the scalp normal matters as well, since it determines the direction in the cortex of the induced electric field,

which is approximately tangential to the head surface. This third degree of freedom in orientation is often chosen so that the induced electric field is perpendicular to the targeted gyrus.

### Limits of targeting

In TMS, the field strength and thus physiological effects decay with distance from the coil. Particularly with common focal coils, already small tilts with respect to the optimum tangential placement result in attenuation of the maximum field strength (Opitz et al. 2013; Schmidt et al. 2015). Real-time navigation allows for maintenance of the proper tangential placement of the coil with respect to the head of the subject, with the focus point of the figure-of-eight coil, which in many coils corresponds to the coil center, touching the scalp. Maintaining the coil placement to be tangential to the scalp is sometimes overlooked and can be challenging, especially for inexperienced operators. Instead of placing the focus point of a figure-of-eight coil on the head surface (maintaining correct pitch), operators tend to touch the head with a point closer to the coil handle; left-right misalignment (roll) seems to be easier to control (see Figure 7.1). Some neuronavigation systems therefore detect and display the orientation error but require correct registration and, more importantly, operator awareness of this issue (see the crosshairs in the lower right corner and the arrows representing the orientation of the stimulation transducer in the 3D display of Figure 7.2). The orientation issue is aggravated in focused ultrasound stimulation, which can reach deeper structures than the rather superficial TMS.

Neuronavigation systems without robotic positioning only measure and report positions and/or errors relative to a selected target. Typically, these measurements are used as a visual feedback for the operator to minimize the actual deviation from a specific position. Most available systems can also record the six degrees of freedom of the coil position in the head coordinate system for each stimulus if the stimulator's trigger output is connected with a trigger input of the navigation system and the triggered recording setting is activated. Recorded position data allow post-hoc analysis. In combination with computational and/or empirical statistical models, such post-hoc analysis can not only document the actual coil locations for quality control and reporting, it can also correct output fluctuations, e.g., of motor evoked potentials (MEP), due to coil position fluctuations to reduce unaccounted variability and increase accuracy in excitability measurement procedures.

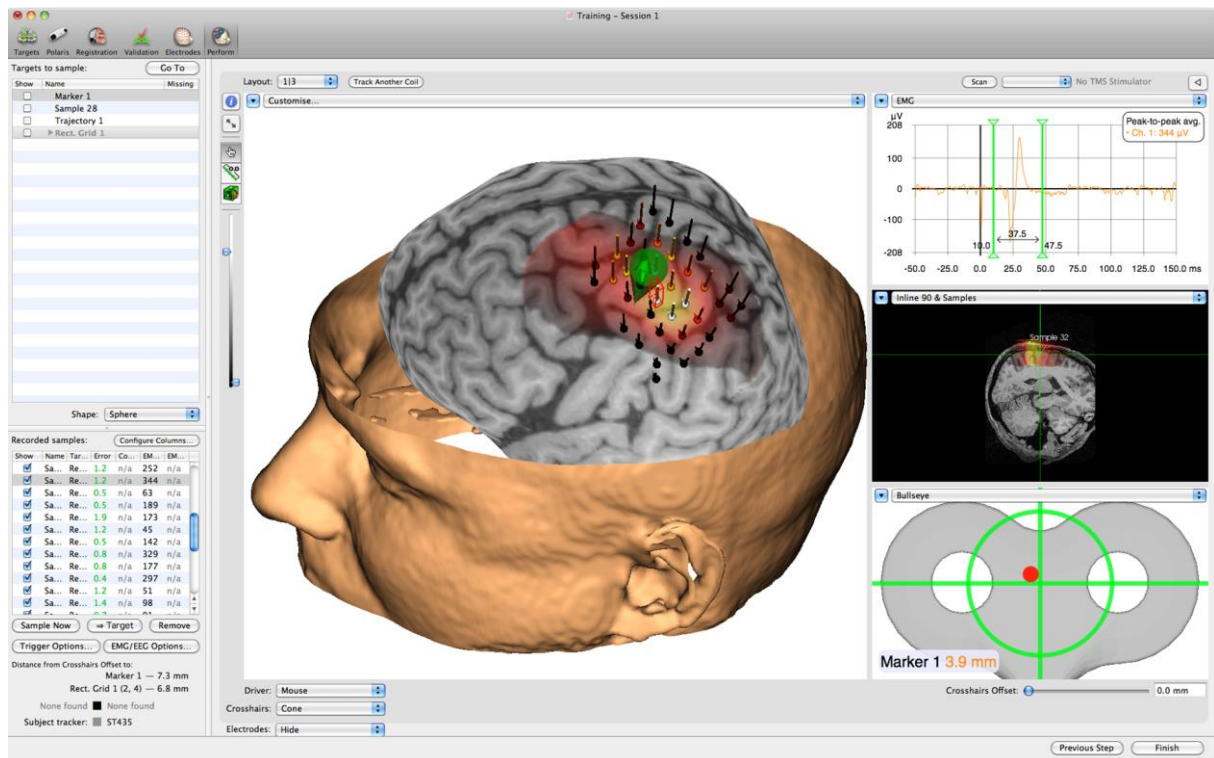


**Figure 7.2 about here**

**Caption:** User interface of a typical neuronavigation system (courtesy of Rogue Resolutions Inc.) with 3D view (center), position as well as electromyography recordings per sample (bottom left panel), electromyography trace (top right), slice view (middle right), and bullseye view with orientation information (bottom right).

## Target identification

An important part of neuronavigation is target identification. With stimulation methods evoking action potentials, such as TMS, only a few cortical regions can be located by a directly observable response or acute disruption of certain observable brain functions. Most prominent among these are the primary motor cortex representations of small hand and other peripheral muscles, which respond to suprathreshold stimulation with twitching. This response can be detected through electromyography and is also visible for sufficiently strong stimuli (Volz et al. 2015; Westin et al. 2014). Although experienced operators may quickly find representations of many muscles with suprathreshold stimulation in the primary motor cortex, similar or moderately increased stimulation amplitudes can also generate motor evoked potentials in more anterior targets outside the primary motor cortex (Teitti et al. 2008).

Other cortical areas that can be located through relatively simple observations are the somatosensory cortex, where the perception of peripheral pain stimuli near the sensation threshold can be suppressed; the visual cortex, where neurostimulation elicits phosphenes and/or shortly interrupts visual perception; and the speech area, where short stimulus trains cause speech arrests (Oliver et al. 2009; Hannula et al. 2005; Kanda et al. 2003; Kammer, Beck, Erb, et al. 2001; Amassian et al. 1989; Devlin and Watkins 2007; Pascual-Leone, Gates, and Dhuna 1991). Through similar effects—though typically with higher variability and lower retest stability—access points to the corticovagal circuit can be located in the prefrontal cortex through bursts that act on the autonomic nervous system and change the heart rate and/or heart rate variability (Makovac, Thayer, and

Ottaviani 2017; Iseger et al. 2017; Iseger et al. 2020; Kaur et al. 2020; Michael and Kaur 2021).<sup>3</sup> The stimulation of several other cortical areas can specifically disrupt certain cognitive functions (Oliver et al. 2009; Hannula et al. 2005; Kanda et al. 2003; Ro, Farnè, and Chang 2002). Experiments suggest that further targets can be located through their functional connectivity to a site with detectable responses by stimulating at both locations and shifting the threshold; an example is gating phosphenes, but this paradigm is complex and prone to variability, so it is rarely used (Amassian et al. 2008).

Based on a detectable and, ideally, quantifiable response to a single stimulus or a stimulus train, an operator can approach the target iteratively, maximizing the response (Wilson, Thickbroom, and Mastaglia 1993; Meincke et al. 2016). Such iterative methods solely based on feedback optimization, sometimes called hot-spot search, have the advantage that, in principle, they converge to the perfect targeting parameters, typically position and orientation of the stimulation transducers. The procedure requires minimum assumptions about the focus location or spread of the specific stimulation technology and does not rely on a spatial model of the underlying physics or a detailed definition of the neural target.

Aside from these few examples, however, the majority of brain targets are *silent*, as they do—with currently available detection techniques and/or low enough variability for intra-individual testing—not produce a readily observable response. These targets can be identified in various ways, sometimes contradicting each other. These approaches typically involve the identification of anatomical or functional features in the cortex (Figure 7.3). Still, gyral anatomy is not visible and functional organization is even less accessible. Thus, in addition to the identification of an anatomical or functional target, the target location must be registered in a noninvasively accessible coordinate system.

At the population level, anatomical and some functional targets have been defined empirically and documented in brain atlases. These allow the estimation of distances to reference points. Most prominent is the so-called *five-centimeter rule* (often extended to 6 cm for a more anterior target; see below) that estimates the location of the dorsolateral prefrontal cortex, as a target for depression treatment, to be 5 cm anterior to the hand representation in the primary motor cortex (Lisanby et al. 2008; George et al. 2010). Similarly, the premotor and the primary somatosensory cortices have been targeted relative to the primary motor cortex (Rizzo et al. 2004; Gerschlager, Siebner, and Rothwell 2001; Koch et al. 2006). However, absolute distances from a reference do not account for individual anatomical differences, not even head size. In comparison, the international 10–20 coordinate system, which is used widely in electroencephalography (EEG) (Jasper 1958), scales with the head dimensions and therefore provides more individualized relative distances (Herwig, Satrapi, and Schönfeldt-Lecuona 2003; Seyal, Masuoka, and Browne 1992; Walsh et al. 1998). Approaches defining the target relatively between head landmarks, such as the nasion–inion line, are applied in therapy as well as in research and resemble the 10–20 system (Walsh et al. 1998; Levkovitz et al. 2015; Mir-Moghtadaei et al. 2015). The 10–20 and related systems can be combined with individual imaging data and may serve as a navigation tool without stereotaxy (Wassermann et al. 1996; Weiduschat et al. 2009; Andoh et al. 2009; Paillère Martinot et al. 2010). However, stereotactic neuronavigation, as described in more detail later in this chapter, can further refine the referencing of scalp surface to head imaging data (registration) (Neggers et al. 2004).

---

<sup>3</sup> Repetitive TMS at this target has also shown an impact on cortisol and stress regulation, whereas heart-rate variability measures were not significant in this study, indicating the large fluctuations of this effect (Pulopulos et al. 2020).

Instead of population data of anatomy or functional organization from brain atlases, individual brain scans, such as computed tomography (CT), magnetic resonance tomography (MRI), functional MRI (fMRI), or positron emission tomography (PET), promise higher accuracy (Volz et al. 2015). T1-weighted MRI scans currently dominate anatomical target identification. For functional information, subjects usually perform a specific task during a scan so that 3D activation maps can be collected together with anatomical data to serve for subsequent individual targeting. Targets within such widespread areas as the prefrontal cortex may also be identified through their functional connectivity profile (Weigand et al. 2018).<sup>4</sup> Although functional imaging is ideally performed prior to stimulation on an individual level, the identification of a target is often based on inference statistics of group data including brain normalization procedures, i.e., the individual brain 3D coordinates are transformed into the normalized Montreal Neurological Institute (MNI) or Talairach spaces for averaging. A target location reflects maximum activity of a given task on the group level without consideration of individual variability in cortical gyration. This group mean, or even an average taken from several studies, the so-called probabilistic target identification approach (Paus et al. 1997), subsequently serves for coil positioning, corrected by transforming it back into the individual brain coordinates. Two seminal studies compare a number of different targeting approaches (Sack et al. 2009; Sparing et al. 2008). Sack and colleagues demonstrated in a cognitive task that the use of the individual functional architecture yields stronger behavioral effects from stimulation compared to navigation based on group functional results, as well as navigation based on anatomical landmarks. The weakest effects were obtained by placing the TMS coil based on scalp coordinates following the 10–20 system. The statistical power in the study significantly increased when the targeting was based on the approaches in the following order: 10–20 system, group-fMRI, individual anatomical MRI, and individual fMRI. Sparing and collaborators found a similar relationship for the hand representation in the primary motor cortex, with the caveat that individual fMRI-guidance could not reach the same amplitude of motor evoked potentials as an individual iterative hotspot search. Similarly, De Witte et al. (2018) demonstrated that the electrode placement in electrical stimulation for depression treatment as well as the consequential electric field distribution according to the 10–20 system significantly deviates from the positions chosen if individual anatomical imaging data were considered.

Depression treatment may be a good example how these various general techniques have been explored. Initially, an unfocal round TMS coil was used, often simply placed centrally, i.e., approximately on Cz in the 10–20 system (Höflich et al. 1993; Kolbinger et al. 1995). Subsequently, figure-of-eight coils with increased focality were targeted to Brodman Areas 9 and 46 or the interface in between (Mayberg 1997; Fitzgerald 2021). However, these areas are still relatively large compared to the TMS coil focus and are spatially and functionally variable across individuals.<sup>5</sup> In consequence, a coil placement definition relative to the motor representation of the hand in the five-centimeter rule provided a simple method, which became the basis of the first clinical approval studies (Lisanby et al. 2008; Pascual-Leone et al. 1996; George et al. 1997). With time, the five centimeters got extended to six for more anterior stimulation, which was found to lead to better treatment outcomes (Herbsman et al. 2009). The unreliability of the five-centimeter rule in targeting was discussed early on, including lack of proper accounting for the patient’s head size (Gershon, Dannon, and Grunhaus 2003). These

---

<sup>4</sup> In addition to the dorsolateral prefrontal cortex, researchers have targeted various circuits based on connectivity for cognition research and clinical applications (Esterman et al. 2017; Tambini, Nee, and D’Esposito 2018; Raji et al. 2018; Momi et al. 2021). Applicable connectivity between nodes in a circuit is often detected through functional imaging, diffusion-tensor imaging, or EEG, including TMS–EEG (Weigand et al. 2018; Koch et al. 2018; Tao et al. 2020).

<sup>5</sup> It is noteworthy that K. Brodmann separated areas based on their neuronal organization differences emerging in histology, resulting in relatively large structures with sometimes gradual transitions in between, no function-based definition, and sometimes diffuse spatial outline that can vary between individuals (Brodmann 1909).

shortcomings led to the development of various anatomical targeting strategies from structural images (Mylius et al. 2013) and simplified methods referenced to the skull/scalp in 10–20 coordinates, for example coil placement on the F3 position, which is also the basis of the procedure behind the popular Beam F3 method (Mir-Moghtadaei et al. 2015; Trapp et al. 2020). The latest targeting methods for depression treatment use functional connectivity, specifically the site with maximum negative correlation with the subgenual cingulate cortex in group analysis and preferably on an individual basis (Fox et al. 2012; Fox, Liu, and Pascual-Leone 2013; Weigand et al. 2018; Cole et al. 2020; Cash et al. 2021). This functional connectivity was reported to coincide with anatomical connectivity, at least in the left hemisphere (Tao et al. 2020). Connectivity-based targeting may increase TMS treatment efficacy (Cash et al. 2019). A recent alternative procedure uses the above-cited effect on the heart rate or heart-rate variability through vagal connectivity, which allows an iterative target search without imaging tools and according to current understanding also involves the subgenual cingulate cortex (Iseger et al. 2017; Iseger et al. 2020; Michael and Kaur 2021). In all cases, individual targeting (e.g., based on structural as well as functional imaging and also connectivity) has demonstrated increased treatment efficacy (Fitzgerald et al. 2009; Cash et al. 2019).

These results contrast with the actual practice of therapeutic TMS in clinics, which predominantly uses simple targeting approaches, ignoring anatomical and functional individuality. This practice risks not only large targeting variability but can also result in stimulation far outside the intended brain areas, which might influence efficacy and suggests revisiting established procedures for brain stimulation (Lefaucheur et al. 2007; Pommier et al. 2017; Ahdab et al. 2010; Mir-Moghtadaei et al. 2015; Mir-Moghtadaei et al. 2016; Schönfeldt-Lecuona et al. 2010; Seibt et al. 2015). However, larger clinical trials are required to demonstrate the superiority of individualized targeting on patient outcome. Comprehensive summaries of the most recent status on targeting for depression treatment are available in the literature (Cash et al. 2020; Fitzgerald 2021).

Conventionally, brain stimulation directly targets the brain region of interest. However, some targets may not be accessible this way, such as subcortical nuclei for TMS. As indicated by the connectivity-based identification of accessible targets, stimulation at one location can cause activation at remote sites, including subcortical targets as deep as the hippocampus or the brain stem (Li et al. 2004; Wang et al. 2014). Transsynaptic targeting and targeting of white-matter tracts actively exploits this mechanism not just to identify a circuit but to stimulate or modulate neural circuits indirectly through a site that the operator would otherwise not consider relevant (Nummenmaa et al. 2014). Individual tractography based on diffusion tensor imaging (DTI) can support the identification of such indirect stimulation pathways (Hannula et al. 2010). Similar to target identification based on structural connectivity, indirect targeting can be alternatively based on functional connectivity between brain regions, obtained, for example, with resting state fMRI (Ulrich et al. 2018; Weigand et al. 2018; Fox et al. 2012).

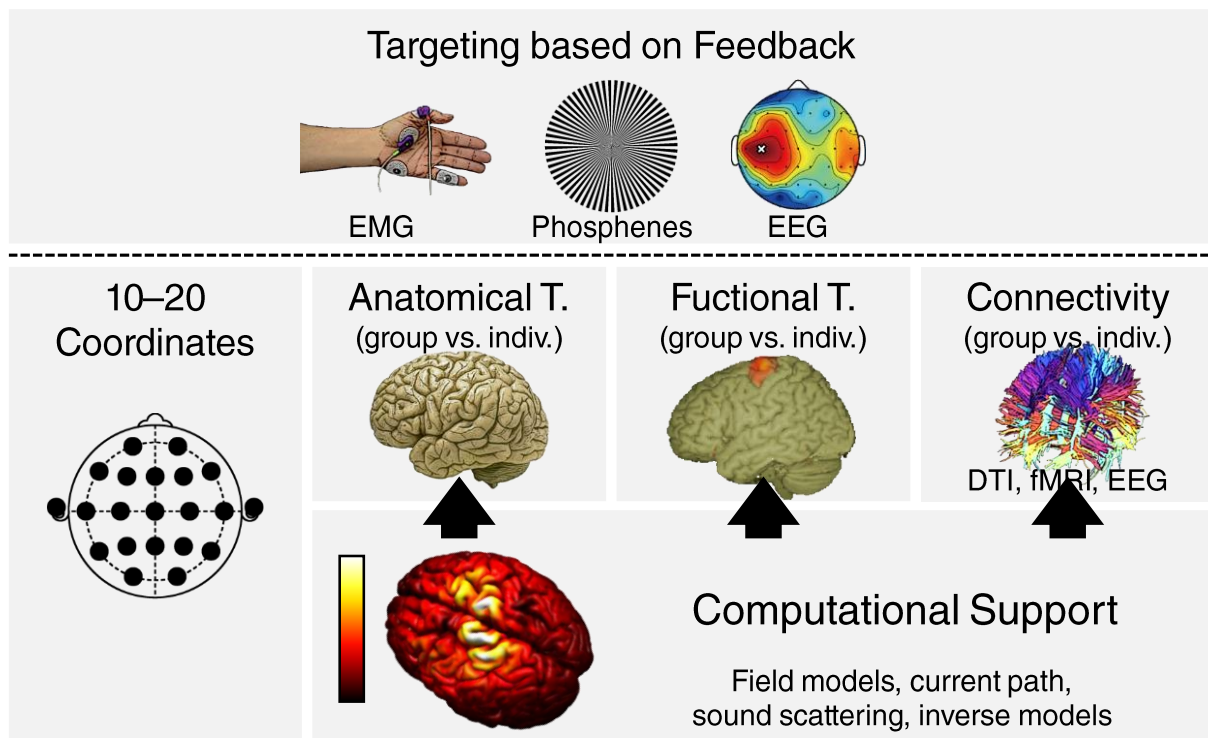


**Figure 7.3 about here**

**Caption:** At present, only a few targets can be located through iterative hot-spot search by maximizing or minimizing feedback (top), most prominently muscle representation in the primary motor cortex. Indirect targeting through skull/scalp-based references (e.g., 10–20 coordinates) or structural, functional, or connectivity imaging can provide access to other targets. In case of imaging data, individual target identification with sufficient statistical power improves the outcome compared to group analyses in the few existing studies. Computational methods increasingly support targeting by optimizing the transducer location and orientation, stimulation amplitude, as well as other parameters in electrical, magnetic, and ultrasound stimulation and modulation.

### Stimulation transducer positioning and maintenance of position

In most interventions across all stimulation techniques, a given stimulation site is to be maintained for a certain time, ranging from minutes to more than an hour. The stimulation transducer (e.g., a stimulation coil), could be fixed on a tripod or could be handheld by an operator. In both cases, small head movements and/or transducer movements result in drifts of the transducer position with respect to the head (Goetz et al. 2018). Navigation systems can provide a means of controlling and documenting this drift. In the case of handheld operation, the transducer position can be iteratively corrected to account for head position drifts, whereas this is more complex and challenging in the case of tripod-mounted transducers. A robot system moving the coil dynamically to compensate for head movements can be a sophisticated but presently expensive solution.

Neuronavigation systems can support brain stimulation interventions in several ways. First, such systems can serve in procedure planning and target identification using functional or anatomical data. Second, neuronavigation can help maintain the stimulation focus on the target during a session by reporting the placement error in real time with respect to the six degrees of freedom (i.e., three translational and three rotational) using the above mathematical formalism. Finally, neuronavigation can help document brain stimulation interventions by recording the position of the transducers,

which aids interpretation and reproducibility of the procedures. For example, two or more consecutive sessions with the same subject or patient often require an identical coil position, which can be stored and reproduced using the neuronavigation system. In this case, anatomical or functional data from subjects are not strictly required, since a generic head model could be used instead. At present, frameless stereotactical neuronavigation systems routinely serve for TMS coil positioning, digitizing EEG or stimulation electrode coordinates, or ultrasound transducer placement in research (Barnett et al. 1993; Beisteiner et al. 2020).

Frameless stereotactic neuronavigation systems were adopted from neurosurgery to measure the position and orientation (six degrees of freedom) of transducers and the subject's head and to derive relative coordinates between them. Various neuronavigation systems developed for neurosurgery or dedicated to transcranial brain stimulation are available on the market.<sup>6,7</sup> Several open-source solutions have been presented in publications as well (Ambrosini et al. 2018; Souza et al. 2018; Rodseth, Washabaugh, and Krishnan 2017).<sup>8</sup>

While presently most of the neuronavigation systems used for transcranial stimulation are optical, magnetic and radio-frequency stereotaxy played a role in early studies (Wassermann et al. 1996; Paus 1998; Bastings et al. 1998; Picht et al. 2009). Such electromagnetic tracking systems are widely used in other fields of medicine and technology, including early neurosurgery, as they do not need a direct line of sight, although they are known to suffer from distortion in the vicinity of magnetic or conductive materials or currents that generate interfering electromagnetic fields in the right spectral range (Franz et al. 2014; Sorriento et al. 2020; Poulin and Amiot 2002). Nevertheless, electromagnetic tracking has recently received regulatory clearance for TMS (Datta 2020).

Early optical neuronavigation systems used in brain stimulation employed active markers (e.g., light sources such as infrared light emitting diodes, LEDs) fixed to spots on the transducers and the subject that do not move relative to the skull (Schönfeldt-Lecuona et al. 2005). These light sources, also called trackers, are monitored by at least two cameras with different, known positions (e.g., in a stereo camera), which can identify the position of an LED by triangulation. Accordingly, through the pixel coordinates each camera can identify a line pointing to the position of the LED in its view; the intersection of both lines provides the position. If the system uses at least three LEDs with known

---

<sup>6</sup> Commercial neuronavigation systems used in brain stimulation are available from (examples in alphabetical order) ANT Neuro (Hengelo, Netherlands), Brain Science Tools (De Bilt, Netherlands), EMS Medical (Bologna, Italy), HHTNK Xi'an Solitaire Brain Control Medical Technology Co. (Xi'an, China), Localite (Bonn, Germany), Nexstim (Helsinki, Finland), Rogue Research (Montreal (QC), Canada), Soterix Medical (New York (NY), USA), and Storz Medical (Tägerwil, Switzerland). Several commercial systems primarily for neurosurgery from Brainlab (Munich, Germany), Medtronic (Minnesota (MN), USA), Stryker Navigation (Kalamazoo (MI), USA), and Zeiss Medical (Jena, Germany) have been used for brain stimulation as well.

<sup>7</sup> Most available neuronavigation setups do not use a custom-designed tracking component but build upon available solutions from third parties to perform triangulation. Suppliers for optical infrared tracking platforms include Northern Digital (Waterloo (ON), Canada), ClaroNav (previously incorporated as Claron Technology, Toronto (ON), Canada), Atracsys LLC (Puidoux, Switzerland), BTS Bioengineering Corp. (Quincy (MA), USA), PS-Tech (Amsterdam, Netherlands), NaturalPoint with the brand OptiTrack (Corvallis (OR), USA), Qualisys AB (Göteborg, Sweden), PhaseSpace (San Leandro (CA), USA), Vicon Motion Systems Ltd. (Oxford, UK), and Ultraleap Ltd. (Bristol, UK). The former four have a strong focus on medical procedures; the latter are used in film-production motion tracking, industry applications, and biomechanics. The FreeTrack project provides a mostly open-source optical tracking software application and library similar to the commercial systems, operating with a wide range of consumer-grade and professional cameras. Such systems could in principle bring down the cost of neuronavigation, but a brain-stimulation application layer and a standardized setup for controlled accuracy and/or calibration are yet to be developed.

<sup>8</sup> Most prominent among the open-source solutions specifically for brain stimulation are StimTrack, which builds upon the open InVesalius software package, and NeuRRoNav (Ambrosini et al. 2018; Souza et al. 2018; Rodseth, Washabaugh, and Krishnan 2017).

relative position to each other on an object and if they are not collinearly arranged, the system can measure the orientation of the object based on the distance of each of the three LEDs (Zhou et al. 2017). If multiple LEDs such as triples with different positions of the individual LEDs to each other are used, the system can identify each of the triples, for example, subject versus stimulation transducer or various transducers. LEDs further allow modulation of the light signal to encode and communicate further information or to identify them individually. However, active light sources such as LEDs require power, typically delivered through cables, which can move or detach the LEDs due to the cables' weight or get in the way of other equipment. Instead, most modern frameless stereotactic neuronavigation systems use retroreflective trackers, known from cat's eye bike reflectors and road markings, which are illuminated by external light sources (typically infrared) located around the cameras. If the reflective trackers are shaped like small balls, they are visible from almost all directions and maximize the detectable positions of the subject and transducers (see Figure 7.4). However, as the trackers are covered with fine glass beads to generate the retroreflective effect, they are very sensitive to abrasion and dirt, and should therefore not be touched.

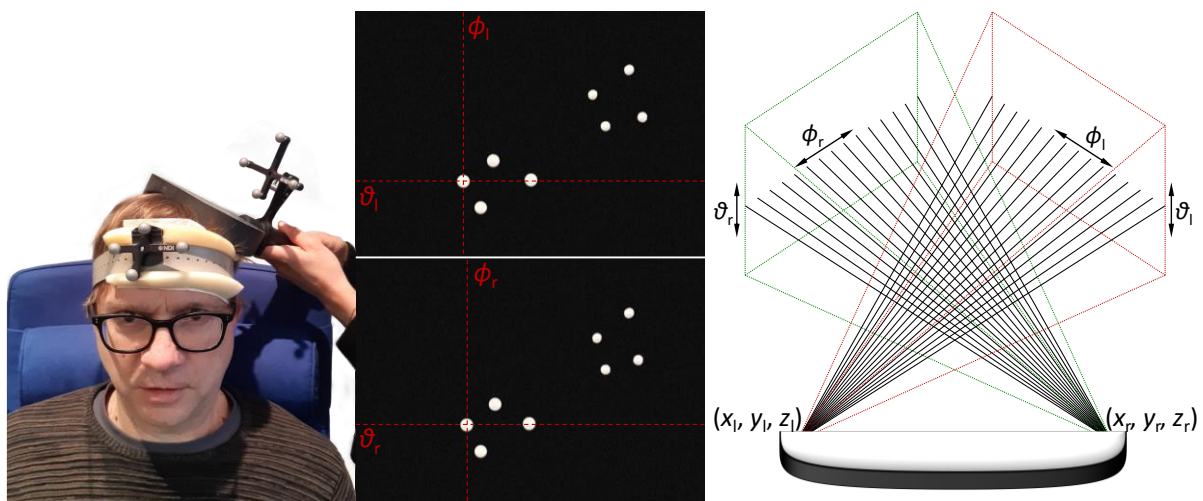


**Figure 7.4 about here**

**Caption:** Retroreflective markers mounted on a subject's forehead and a TMS coil (left). The subject tracker is fixed via an almost inelastic and wide band and without a post that could form a long lever. Glasses (see Figure 7.8) could further stabilize the position and are less susceptible to face muscle activity. At least two cameras detect predominantly the retroreflective balls in their view as their brightness in response to the infrared light sources near the camera axes outshines any other object under typical in-door light conditions (middle). With exact knowledge of the positions of the left  $(x_l, y_l, z_l)$  and right  $(x_r, y_r, z_r)$  cameras, either through calibration or as they are mounted to a fixed camera beam, software can interpret each pixel location as a spherical angle  $(\phi_l, \vartheta_l)$  and  $(\phi_r, \vartheta_r)$  and estimate the position of corresponding light spots in 3D from it (right). The comparison of the relative geometric position of the individual balls with reference arrangements (typically three or four balls) allows the identification of different trackers to single out the subject's and one or several instruments' positions.

Infrared cameras<sup>9</sup> with strong light sources that are mounted closely, e.g., coaxially with the cameras, see practically only the retroreflective markers in their images, which appear as bright,

<sup>9</sup> Typically those cameras use normal complementary metal-oxide-semiconductor (CMOS) or charge-coupled device (CCD) sensors, as in digital consumer cameras, with filters for the visible spectrum and are therefore mostly sensitive to near-infrared light.

almost saturated pixels on a relatively dark background (see Figure 7.4). These images allow relatively simple processing either as binary bit maps after thresholding luminosity (i.e., strictly black and white) or as grey-scale pictures with few gradation levels to allow for subpixel position estimation. The spherical shape of the markers leads to identical projections from any angle and allows simple estimation of their center from each perspective if the line of sight is not covered unfavorably or a large portion of a ball shadowed. The computationally fastest method for estimating the center of a ball may be calculating the first-order moment by taking the average of the pixel positions of contiguous white spots—weighted with the pixel value if not thresholded—but can introduce bias for partial coverage of a ball. Maximum-likelihood or similar regression of a round outline can improve performance at the cost of speed. Closely related are vote-based search methods such as the Hough transformation, for which faster derivations are available (Yuen et al. 1990; Wu et al. 2019).

Sunlight and other sufficiently strong infrared light sources can confuse such simple processing but are rarely present in brain stimulation laboratories. If the geometric position of the two individual cameras is fixed relative to each other, no further calibration of their reference frame is required. Each pixel of the images collects light from sources within a sharp spherical angle so that each pixel lighting up in one camera image represents an axis on which the corresponding ball is expected. Since the axes of the two cameras intersect, the 3D position of each ball and thus also their center is well defined in the camera coordinate system, i.e., relative to the camera positions, through triangulation (Hartley and Sturm 1997). From the 3D positions of the individual balls, the trackers with their specific unique geometric arrangement of balls can be tested with maximum likelihood and similar techniques against all stored geometric arrangements to identify the trackers of specific subjects and transducers.

Ideally, the camera is close to the normal of the plane spanned by three or more balls and can clearly differentiate them. In the worst case, two balls are located collinearly on or near a camera axis. Then, the two balls become indiscernible to the stereo camera and the accuracy of the position estimation may suffer. As soon as the images of two balls—also balls from different tracker—touch each other, some systems can have problems separating them into individual balls.

For the triangulation of markers, the corresponding location of each marker has to be identified in every camera image. Present mathematical descriptions typically do not just interpret every camera pixel by its two angles (see Figure 7.4), but represent the problem through projection equations. In turn, they can also compensate imperfections; for example, lens aberration and other distortion of the camera system can be corrected if an invertible prior camera characterization is available. Each camera projects the three coordinates of a point in space, e.g., of a retro-reflective marker  $\mathbf{r} = (x, y, z)^T$  in world coordinates into two projected coordinates  $(\phi_i, \vartheta_i)^T$  in the image plane of each camera  $i$ . For two cameras in a stereo setup—one on the left, one on the right ( $i \in \{l, r\}$ )—the overall equation reads

$$\begin{aligned} \begin{pmatrix} \phi_l \\ \vartheta_l \end{pmatrix} &= \mathbf{P}_l \circ \mathbf{T}_l \left( \begin{pmatrix} x \\ y \\ z \end{pmatrix} \right) \text{ and} \\ \begin{pmatrix} \phi_r \\ \vartheta_r \end{pmatrix} &= \mathbf{P}_r \circ \mathbf{T}_r \left( \begin{pmatrix} x \\ y \\ z \end{pmatrix} \right), \end{aligned} \tag{1}$$

with the 3D–2D projection functions  $\mathbf{P}_l$  and  $\mathbf{P}_r$  ( $\mathbb{R}^3 \rightarrow \mathbb{R}^2$ ) of the left and right cameras and the camera's individual geometric transformations  $\mathbf{T}_l$  and  $\mathbf{T}_r$  ( $\mathbb{R}^3 \rightarrow \mathbb{R}^3$ ) from the same world coordinates to the individual camera location and perspective. Without any individual camera distortion, the

projections  $\mathbf{P}_l$  and  $\mathbf{P}_r$  are identical since the geometric conditions of the cameras and their individual relations to the world origin are exclusively represented by the geometric transformations. Whereas the projection mappings are linear, the geometric transformations include rotation and translation to account for the different camera locations as well as perspectives, and accordingly are affine mappings. Using the four-dimensional representation described below, the affine mappings can be linearized and turned into homomorphisms, each represented by a matrix.

The triangulation equation system (1) has to be solved for  $(x, y, z)^T$  based on the detected and known pixel coordinates in the camera projections  $(\phi_l, \vartheta_l, \phi_r, \vartheta_r)^T$ . Accordingly, it is typically over-defined by at least one degree of freedom—at least two camera projection pictures with two degrees of freedom each to measure the three degrees of freedom of a marker (e.g., a retroreflective ball or pad) in space. Accordingly, the matching has in most cases one best-fitting solution. Sometimes, however, matching of individual trackers in the various camera images can cause problems and lead to ambiguity, particularly with many of trackers in view, where the chances increase that the camera positions and more than one marker are in the same plane (camera–marker coplanarity) (Yan et al. 2014).<sup>10</sup> An incorrect matching leads to so-called ghost images or ghost marker locations, where the system assumes a wrong position for a reflector. The inclusion of additional information and constraints can turn this matching problem into a constrained tree-search task. First, the individual markers on one tool typically have known geometric relationships, which can rule out ambiguity in matching (Liere and Mulder 2003). Furthermore, the silhouette, specifically the size of the outline of the retroreflective markers in the camera projections, can reduce the risk of wrong matching (Lin et al. 2018). As soon as the trackers associated with a specific object are identified and located, the corresponding object can be represented in 3D with its exact outline, position, and orientation if the object’s outline, e.g., a 3D model of it, has been registered relative to the trackers before.

Mathematically, stereotaxy has strong ties to computer graphics and computer vision. With retroreflective markers and strong infrared light sources, stereotaxy systems generate a scenery largely independent from the visible world and do not need complicated object recognition or anatomical feature detection, though such functions might improve neuronavigation systems in the future. Instead, triangulation of the markers provides the location of the head frame as well as the tool frame, both in six degrees of freedom with a position vector  $\mathbf{p}$  and the orientation matrix  $\mathbf{O}$  in the world coordinate system,

$$\begin{aligned} \mathbf{r}_p &= \begin{pmatrix} x_p \\ y_p \\ z_p \end{pmatrix} \text{ and} \\ \mathbf{O} &= \mathbf{O}_{\text{roll}} \mathbf{O}_{\text{pitch}} \mathbf{O}_{\text{yaw}} = \begin{pmatrix} 1 & 0 & 0 \\ 0 & \cos \alpha & -\sin \alpha \\ 0 & \sin \alpha & \cos \alpha \end{pmatrix} \begin{pmatrix} \cos \beta & 0 & \sin \beta \\ 0 & 1 & 0 \\ -\sin \beta & 0 & \cos \beta \end{pmatrix} \begin{pmatrix} \cos \gamma & \sin \gamma & 0 \\ \sin \gamma & \cos \gamma & 0 \\ 0 & 0 & 1 \end{pmatrix} \\ &= \begin{pmatrix} o_{11} & o_{12} & o_{13} \\ o_{21} & o_{22} & o_{23} \\ o_{31} & o_{32} & o_{33} \end{pmatrix}, \end{aligned} \quad (2)$$

where  $\alpha$ ,  $\beta$ , and  $\gamma$  are the roll, pitch, and yaw angles, respectively.<sup>11</sup> These vectors and matrices represent the transformation necessary to bring the head, stimulation transducers, or other tools

<sup>10</sup> In the case of such camera–marker coplanarity of two or more markers, these markers share at least one coordinate in the camera projections so that the over-definition is gone and their camera images mutually fulfill the triangulation equations.

<sup>11</sup> The order of the individual rotations changes the outcome as rotations in three dimensions do not commute. Any of the six different possible orders of rotations can be used in a system with correct results if the initial definition is used consistently.

from their generic origin positions to the detected positions so that each point on a specific object  $\mathbf{p}_o = (x_o, y_o, z_o)^t$  undergoes the transformation

$$\begin{pmatrix} x \\ y \\ z \end{pmatrix} = \mathbf{O}_{\text{roll}} \mathbf{O}_{\text{pitch}} \mathbf{O}_{\text{yaw}} \begin{pmatrix} x_o \\ y_o \\ z_o \end{pmatrix} + \begin{pmatrix} x_p \\ y_p \\ z_p \end{pmatrix}. \quad (3)$$

The matrix  $\mathbf{O}$  and the translation vector  $\mathbf{r}_p$  are generated for every tracker by the stereotaxy camera and sent to the neuronavigation software. Typically, the neuronavigation software eliminates the world coordinate system as soon as a subject's or patient's head is registered relative to the respective tracker and represents every other object relative to that, i.e., through vector subtraction. Given a target point  $\mathbf{r}_t$  with three degrees of freedom and the closest point on the scalp to that point, an axis can be added so that the software can calculate and display the deviations in position and orientation of a stimulation actuator with known stimulation characteristics, e.g., a focus point on the coil surface.

Often, translation and rotation are combined in a four-dimensional matrix–vector formalism so that the affine mapping of Equation (3) turns into a purely linear transformation,

$$\begin{pmatrix} x \\ y \\ z \\ 1 \end{pmatrix} = \begin{pmatrix} o_{11} & o_{12} & o_{13} & x_p \\ o_{21} & o_{22} & o_{23} & y_p \\ o_{31} & o_{32} & o_{33} & z_p \\ 0 & 0 & 0 & 1 \end{pmatrix} \begin{pmatrix} x_o \\ y_o \\ z_o \\ 1 \end{pmatrix}. \quad (4)$$

The added last dimension<sup>12</sup> serves merely as an auxiliary dimension for a consistent and closed incorporation of the sum and the orientation. Of the 16 entries in the  $4 \times 4$  matrix, only six degrees of freedom are used. Consequently, the entries are highly constrained.<sup>13</sup> The matrix fully describes the position and orientation of a tool and can be recorded in response to a trigger in most modern neuronavigation systems, e.g., for each administered stimulus. Typically, the neuronavigation software can export the individual elements of the matrix of Equation (4) in text format for storing the transducer position and orientation relative to the head and for post-processing.

Alternatively, the problem can be described in quaternions, i.e., Hamilton's four-dimensional complex division ring  $\mathbb{H}$ , which bring about substantial speed advantages and gimbal definiteness (Hamilton 1844-1850; Pletinckx 1989; Goldman 2011). With  $\mathbf{i}^2 = \mathbf{j}^2 = \mathbf{k}^2 = -1$  and antisymmetric commutation of the pairwise products of the imaginary elements  $\mathbf{i}$ ,  $\mathbf{j}$ , and  $\mathbf{k} \in \mathbb{H}$ , numbers are formed of a scalar and a vector part. The location of a point in space can be represented by a number with vector part  $\mathbf{r} = \mathbf{i}x + \mathbf{j}y + \mathbf{k}z$  only and a rotation with angle  $\zeta$  around a normalized axis  $\mathbf{a} = \mathbf{i}a_x + \mathbf{j}a_y + \mathbf{k}a_z$  turns into  $(\cos \zeta/2 + \sin \zeta/2 \mathbf{a}) \mathbf{r} (\cos \zeta/2 + \sin \zeta/2 \mathbf{a})^*$ , where  $*$  denotes the complex conjugation operator. Details on the use of quaternions for three-dimensional geometry in general and the use in medical navigation in particular as well as their relationship with vector analysis can be found in the literature (Pletinckx 1989; Chou 1992; Goldman 2011; Benjema and Schmitt 1998).

Combining the estimated coordinates of the stimulation transducers relative to the head with the computational power of modern computers, almost all available stereotactic systems for brain stimulation can display the monitored scene in 3D as well as several slice representations in real time

<sup>12</sup> Sometimes, the additional dimension is equivalently added as the first dimension by circularly shifting the columns and rows in the matrices and the vectors.

<sup>13</sup> The unused  $16 - 6 = 10$  degrees of freedom (DOF) are: scaling in each of the three dimensions (3 DOF), reflection with respect to three planes (3 DOF), and a zero constraint on the fourth, auxiliary coordinate, fixing the four remaining DOFs.

and overlay them with actual brain scan data of the subject after co-registration (see Figure 7.2). The brain data can be both structural scans as well as activation maps computed from fMRI or PET.

### Technical limitations of neuronavigation

The deceptive perfection of neuronavigation pictures and the apparent precision of the reported coordinates conceal several important limitations. Stereotaxy only measures the positions of trackers, such as retroreflective balls, in space and establishes a coordinate system, but does not automatically know where the head is. Instead, the subject's head and the brain within have to be registered in that coordinate system. Thus, the operator has to link several points of the subject's physical head with their counterparts on the virtual head model, imaging data, or other anatomical datasets within the neuronavigation software each time the head trackers are mounted or relocated. The procedure requires distinct anatomical points that can be identified easily and unambiguously both in the anatomical dataset and on the subject. Furthermore, these points have to be small and confined enough to avoid a large spread in identifying their location. Errors in the latter detract directly from the accuracy of the neuronavigation procedure. As the head has few sharp anatomical landmarks that are accessible noninvasively, are clearly visible in imaging data, and are relatively stable with respect to the skull, locating corresponding points on the head and in the virtual dataset can easily spread by 5 mm (Soteriou et al. 2016; Woerdeman et al. 2007; Pfisterer et al. 2008; Stieglitz et al. 2013; Mascott et al. 2006; Golfinos et al. 1995; Wang and Song 2011).<sup>14</sup> Although a minimum of three points is mathematically sufficient to register a physical head with its imaging data, it is highly recommended to use more than three points to average out the error of the registration.<sup>15</sup> Frequently selected anatomical features are the intertragic notches<sup>16</sup>, the canthi, and the nasion (Kammer, Vorweg, and Herrnberger 2007). To avoid the dependency on a few registration points, sampling of the scalp surface with a pointer or laser scanner was suggested (Noirhomme et al. 2004; Hironaga et al. 2018). As soon as imaging data are co-registered with the physical head, the neuronavigation system can display the positions of all instruments that bear trackers and whose geometry is known to the system, such as pointer tools and stimulation transducers, on the 3D virtual head image overlaid with the anatomical and/or functional data.

The precision and accuracy of locating the reflective trackers are often assumed to determine the performance of a frameless stereotactic system.<sup>17</sup> However, in actual setups for brain stimulation,

---

<sup>14</sup> These studies furthermore show that the error for bone screws and even surface markers, as preferred in neurosurgery to match locations between the head and the imaging data, is typically less than about a third of that of anatomical landmarks.

<sup>15</sup> The error decreases approximately with  $1/\sqrt{n}$  for uncorrelated random errors and no bias, i.e., without systematic error that introduces such bias, where  $n$  is the number of registration points.

<sup>16</sup> Alternatively, the superior end of the tragus where it touches the helix provides a distinct feature. Further, the preauricular point on each side of the head is often cited in the literature, which is situated slightly anterior and is located where a horizontal axis running through the superior end of the tragus reaches the posterior end of the zygomatic arch on each side. This point would technically sit on a bone for a stiff support, but is in practice hard to identify reliably.

<sup>17</sup> The technical accuracy of triangulation and marker localization is considered sufficiently high compared to other error sources for most current optical tracking systems with retroreflective markers (Elfring, de la Fuente, and Radermacher 2010; States and Pappas 2006; Frantz et al. 2003; Wiles, Thompson, and Frantz 2004; Zhou et al. 2017). The American Society for Testing and Measurement released a standardized testing procedure for measuring the technical accuracy of medical stereotactic systems with a focus on surgery in ASTM F2554, which was largely derived from the international standard ISO 10360 for the accuracy of 3D coordinate measuring systems used in engineering and manufacturing. The ASTM F2554 standard includes technical drawings of the required setup. However, the aspects of practical accuracy beyond the marker tracking are not

other factors dominate the error. Whereas the trackers on stimulation transducers can be fixed almost perfectly, those on the subject are more vulnerable to transient or permanent movement. Direct bone mounting, which is ideal from a mechanical standpoint, is not justifiable outside of neurosurgical settings, for which neuronavigation systems were designed originally. Therefore, trackers are typically attached to glasses worn by the subject, stuck to the skin with double-sided tape or adhesive pads such as repurposed electromyography electrodes, or affixed to elastic headbands. If trackers change their position or orientation relative to the head, the entire coordinate system defined by them moves and—even worse for accuracy—rotates. Thus, the operator would stimulate a different location than intended even though all the target error numbers reported by the neuronavigation software appear to be negligibly small.

In the case of temporary tracker displacement, the trackers return to their original position and the error leads to variability in the position and orientation data. In the case of permanent displacement, the trackers are typically sliding. Both are often caused by facial muscles, such as the frontalis and the procerus muscles, but can also occur following activity of other musculature. The closer the trackers are to the face or the neck, the less stable the skin position is. Trackers integrated into glasses ideally sit on the nose bone and the auricular sulci—three points that form a relatively wide fixed frame with low orientational tolerance and minimal movement due to facial muscle activity. The stability of the glasses can be improved by securing them with double-sided tape to the bridge of the nose and/or the temples. Trackers that do not rest on a bone structure but only stick to the skin should use the forehead carefully. With every movement of the eyebrows, the operator must expect wrong readings from the navigation system. Headbands tend to perform worst compared to other tracker mounting approaches. They do not have as well-defined positions as glasses and, consequently, small movements would not be obvious to the operator. Additionally, if such movements were to occur, the headband cannot be moved back to a well-defined position. Headbands are held in place by friction promoted by the elastic force of the band and easily slide on the subjects' hair. In fact, the relatively heavy weight of the trackers promotes such sliding. In addition to the weight, the assembly of at least three reflectors is often mounted on a small plastic or metal frame that protrudes from the head for better visibility from various camera perspectives. However, such frames generate a lever and therefore—in response to gravity or any acceleration of the head—a tilting motion around its root point occurs, which the band typically cannot suppress. A tilt of only 5° of the markers near the forehead already shifts the motor cortex by more than 10 mm. Further, subjects tend to touch trackers, either from an unconscious habit to touch or lift glasses or to explore this novel object, despite instructions to avoid doing so. Finally, dependent on the position of the trackers on the head, the operator may touch or push the trackers as well as the mounting (e.g., headband) while positioning the transducers.

In summary, typical stereotactic neuronavigation systems cannot detect any movement of the trackers relative to the subject's head. Moreover, many operators are unaware of the extent and impact of possible tracker movements. Independent sets of head trackers could detect such movements, but existing commercial systems do not offer this feature. Importantly, each set of trackers should be mounted to the head such that its movement is as independent from the other trackers as possible. Such consistency monitoring and cross-validation could eliminate unnecessary targeting errors through proper technical solutions and should be considered in the future.

A comparatively limited but practical method entails repeated checks of the location of the registration points, e.g., intertragic notches, the canthi, and the nasion, relative to the typically drifting head tracker. At least a second measurement of the registration points at the end of a

---

part of this standard to date. Some background information about the standardization and the observation that practical errors can be higher by a factor of ten is also summarized in the literature (Clarke et al. 2010).

session and reporting the drift values appears to be a good practice and is advisable. Still, such consistency check suffers from the problems of registration with features on soft tissue, since the operator can push the tissue with the pointer for each point until the pre-session values can be reached and errors are apparently zero. Therefore, neuronavigation tools would be well-advised to offer a mode for registration check at the end of a session that does not provide any comparison with the initial registration until after the locations are re-registered to avoid bias of the operator. Further, repetition of the point detection, if done without knowledge of previous registration for statistical independence, can average out measurement variability.

Whereas electromagnetic neuronavigation systems can be susceptible to interference and distortion from external electromagnetic sources or magnetic or shielding materials, optical systems need an unobstructed line of sight from every camera to every marker (Poulin and Amiot 2002; Datta 2020). Multi-camera systems with more than two, ideally different perspectives can improve the visibility conditions, allow for partial shading in some perspectives, and trade off certain errors (Dai et al. 2020). To avoid trackers and the associated issues altogether, laser scanning of the scene during a session has been repeatedly considered as an alternative (Richter, Bruder, et al. 2010; Hironaga et al. 2018; Ettinger et al. 1998). Such systems acquire 3D information of all surfaces, including facial and other head features to establish a local coordinate system. However, laser scanning systems still have slower acquisition rates than simple stereo cameras, resulting in limited update rates. Consequently, technology development has concentrated on tracker-based systems.

The improvement of data quality using navigated TMS in motor cortex stimulation has been investigated repeatedly. The comparison of navigated with unnavigated coil positioning and position maintenance yet includes conflicting data concerning MEP reliability. Whereas Gugino et al. (2001); Sparing et al. (2008); Julkunen et al. (2009) observed advantages of neuronavigation in the reliability or size of MEP responses, Jung et al. (2010) did not find differences in the variance of MEPs. However, MEP distributions are non-Gaussian, heteroscedastic, and affected by coil movements in complex ways, which renders extraction of unbiased statistics complicated and suggests caution interpreting such data (Goetz et al. 2014).

### Latest trends in frameless stereotaxy

A major cost driver in optical frameless stereotactic systems is currently the camera. The availability of 3D cameras in consumer and automotive electronics has recently excited interest in low-cost neuronavigation (Rajput et al. 2018; Xiao, Ruan, and Wang 2018; Zhang, Wang, and Lin 2018; Sathyanarayana et al. 2020; Jaroonsorn et al. 2020). Researchers demonstrated that retroreflective trackers can be read out with more affordable cameras and even simple webcams in combination with strong light sources in the visible range (Washabaugh and Krishnan 2016; Rodseth, Washabaugh, and Krishnan 2017). The above-referenced FreeTrack project provides a well-maintained mostly open-source optical tracking library for both consumer-grade and professional cameras in the visible spectrum as well as infrared cameras.<sup>18,19</sup> Optical distortion of low-cost cameras will have to be taken into account, but may be below the practical error sources listed above.

Advancements of computer vision and videometry furthermore promise the elimination of trackers. Demonstrated trackerless methods either detect features such as facial landmarks of subjects without previous registration and are practically unsupervised or match the camera images with

---

<sup>18</sup> FreeTrack General Purpose Motion Tracking Project. <https://www.free-track.net>.

<sup>19</sup> FreeTrack Code Repository. <https://github.com/PeterN/freetrack>.

reference data of the specific subject, e.g., imaging data, through statistical estimation. As for laser scanning, sharp anatomical landmarks on the head are mostly located in the face whereas the hair tends to be problematic as it can move and deform if touched. As a compromise, low-cost consumer cameras can avoid retroreflective trackers but read out distinctive black-and-white patterns similar to quick response (QR) codes on stickers to replace expensive medical infrared stereocameras (Souza et al. 2018; Leuze et al. 2018; Benligiray, Topal, and Akinlar 2019).

In addition, Sathyanarayana, Leuze, and colleagues demonstrated that consumer-grade head-mounted displays previously known from avionics allow a real-time overlay of brain anatomy or functional data with the view of the operator (Sathyanarayana et al. 2020; Leuze et al. 2018). As the data in such augmented reality setups are the same as in more conventional neuronavigation systems with a separate screen, this development primarily aims at the user interface through handling and practicability.

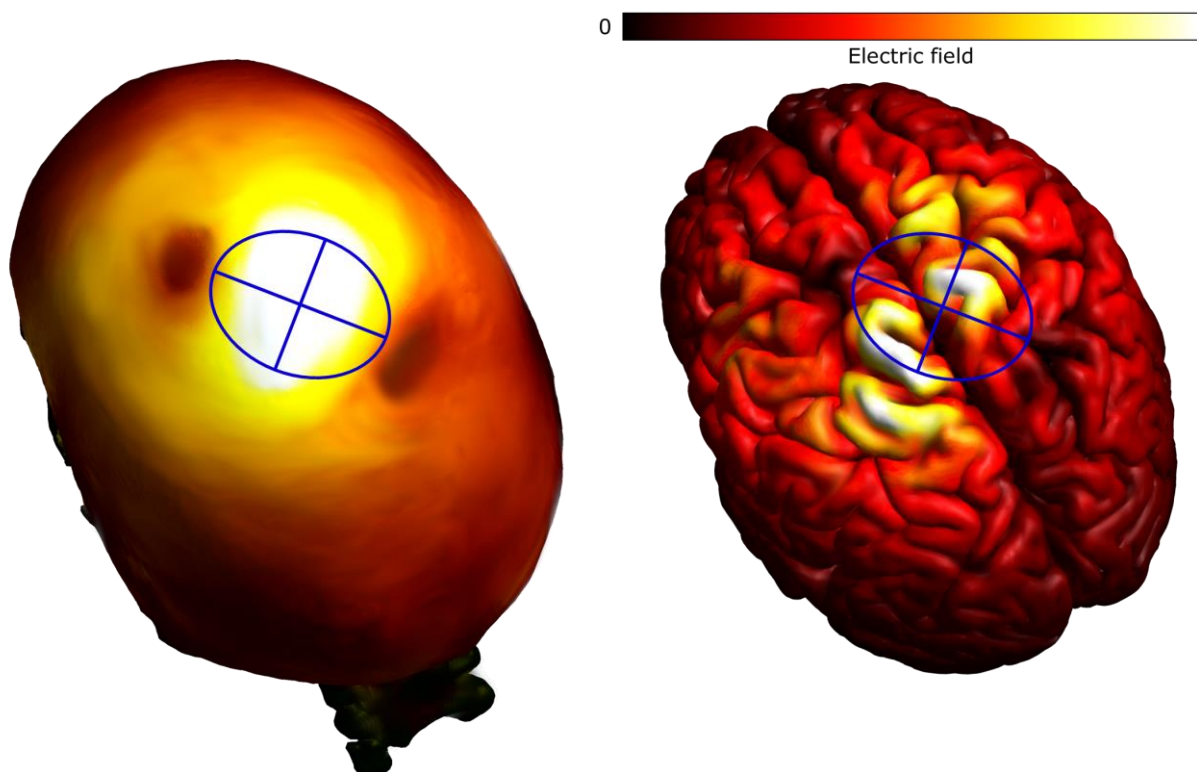


**Figure 7.5 about here**

**Caption:** Electric field model of a figure-of-eight TMS coil with its focus point above the central fissure, highlighting the interaction of electromagnetic induction with the cortical folding (skull depicted on the left and the brain surface on the right). Several gyri relatively remote from the focus point show similarly strong electric fields and have to be considered supra-threshold while there is obviously no target in the central fissure where the focus points.

### Combination of neuronavigation with computational modeling

As pointed out earlier, the assumption that stimulation takes place underneath a well-defined focal point of a stimulation transducer is a substantial simplification as it ignores the interaction of the emitted field with the head tissues. The cortical gyrification and the different physical properties of the scalp, skull, cerebrospinal fluid, as well as brain tissue shift and spread the activated volume for electromagnetic, electrical, and ultrasound stimulation (see Figure 7.5). It is therefore advantageous to use computational modeling to plan the transducers' placement as well as other stimulation

parameters to reach the intended target with maximum focality and minimal transducer energy. Similarly, recorded positions can be used for post-hoc analysis, e.g., to estimate the most likely site of activation, and potential correction of position fluctuations, e.g., in MEP amplitude (Bijsterbosch et al. 2012; Weise et al. 2020).

Simulation models used for targeting range from simple spherical approximations to realistic gyrus-precise models of a representative head template or the individual subject. Although group models appear sufficient, individual anatomic models might offer better accuracy and lower variability, particularly in combination with a target identification on an individual level (Goodwin and Butson 2015; Lee et al. 2015; Stokes et al. 2005; Antonenko et al. 2019; Laakso et al. 2018; Aonuma et al. 2018; Opitz et al. 2013). Studies with TMS over the motor cortex have shown that systematic variation of coil positions in combination with realistic field modelling is able to identify a presumable stimulation site within a gyrus where the calculated field strength is proportional to the measured physiological responses (Laakso et al. 2019; Weise et al. 2020; Bungert et al. 2017). Based on such work, intervention planning can adjust the targeting degrees of freedom, such as the position and orientation of the transducers and the stimulus amplitude, to achieve a specific field strength at the target. Magnetic, electrical, and ultrasound stimulation are often simulated with tools for general physics and engineering problems, which are based on finite element, finite difference, or finite boundary methods, although dedicated tools for brain stimulation have been developed as well (see Chapter 6).

For multichannel electrical stimulation, dedicated software packages are available. Instead of so-called forward modeling (i.e., heuristic and typically manual modification of targeting parameters until a sufficiently good result is achieved), they mathematically optimize current amplitude and polarity for many channels to maximize the field strength in the selected target while minimizing it outside as demonstrated in Figure 7.6 (Dmochowski et al. 2011). Several neuronavigation and simulation tools can also computationally optimize the position and orientation of a single TMS coil to maximize the electric field in a selected target (Gomez-Tames et al. 2018; Gomez, Dannhauer, and Peterchev 2021; Dannhauer et al. 2021).

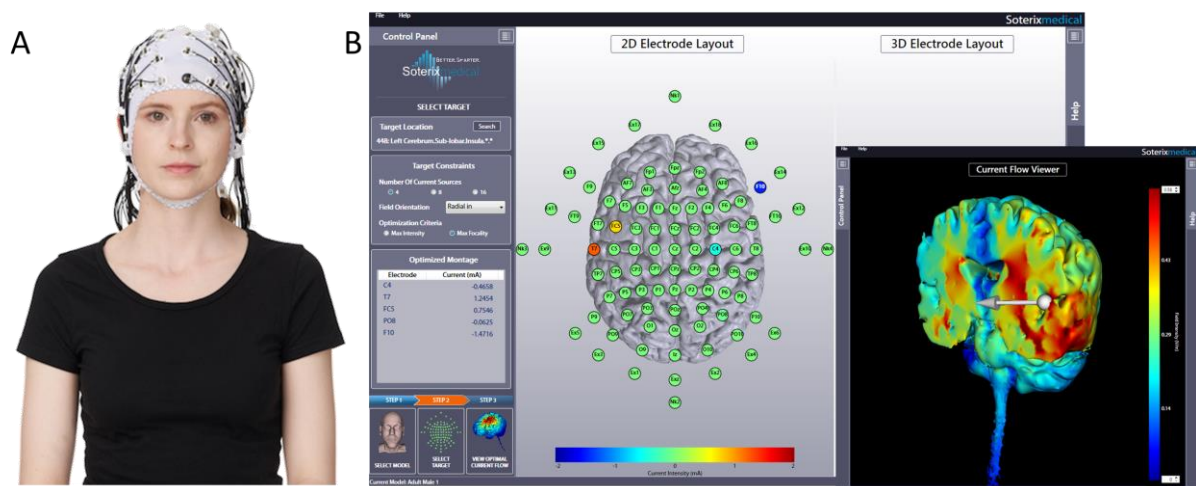


**Figure 7.6 about here**

**Caption:** (A) Multichannel electrical stimulation system and (B) computational intervention planning through electric field modeling in the neuronavigation tool (courtesy of Soterix Medical Inc.).

The techniques described above typically support planning and preparation before a stimulation procedure. The computational solution of realistic high-resolution models used to be on the order of minutes to hours and even mathematical formulations for faster computation have been too slow to enable real-time computation in stereotactic neuronavigation systems (Miranda, Hallett, and Basser 2003; Makarov et al. 2018). For TMS, some commercially available systems estimate the induced electric field online based on simplifications such as a spherical head (Salminen-Vaparanta et al. 2014). However, the gyrification, which is missing in spherical models, is one of the dominant anatomic features that distort the induced electric field (Thielscher, Opitz, and Windhoff 2011).<sup>20</sup> For ultrasound stimulation, especially focused approaches, accurate estimation of scattering and of the locations with highest intensities likewise requires a realistic model (see also Chapter 6 and Chapter 9). With the evolving performance of central and graphics processing units (CPUs and GPUs), online field calculation and visualization have become possible (Laakso and Hirata 2012; Paffi et al. 2015; Stenroos and Koponen 2019). It can be expected that neuronavigation systems will soon not only display the position of the stimulation transducer(s) relative to the brain and overlay it with imaging data, but will also include the physics as well as the physiology, show the field distribution, and even mark the expected stimulated, activated, or modulated volumes in real time.

### Transducer holders

Whereas the above-described targeting methods help select the brain location to be stimulated and the placement of the stimulation transducer(s), the latter still have to be mechanically positioned relative to the brain. In electrical stimulation, adhesive surface electrodes and electrode caps (e.g., according to the 10–20 system) can be fixed on the scalp to provide a relatively stable position with minor influence of facial muscle movement (Villamar et al. 2013; Woods et al. 2016; Bikson et al. 2014); electrode pads fixed with simple straps, however, tend to drift (Woods et al. 2015).

In contrast, TMS and ultrasound typically involve bulky stimulation transducers, such as cooled or iron-core coils or immersion ultrasound transducers with metal casings (Lorenzen and Weyh 1992; Epstein and Davey 2002; Tufail et al. 2011). Manual placement of a TMS coil throughout long sessions requires continuous attention, causes rapid operator fatigue due to the coil weight, and depends on the operator's abilities and experience (Sollmann et al. 2017). Passive mechanical coil holders are common and can, in principle, maintain an initially set coil position throughout a session, given a stable head position (Traad 1990). As the positioning of both TMS and ultrasound transducers involves six degrees of freedom, many holders use articulated arms, i.e., a number of arms series-connected through joints, which are inspired by photography and film technology (Chronicle, Pearson, and Matthews 2005). The joints can provide calibrating protractors to define a coordinate system so that positions can be documented and set based on their coordinates (see also Figure 7.7). However, such conventional mechanical holders are typically cumbersome to stabilize heavy actuators, often show elasticity of their arms as well as joints, and can render accurate adjustments with millimeter accuracy difficult. Counterweights can balance the weight of the stimulation transducer as well as the arm itself and can partially mediate such mechanical problems, but do not solve the issue that passive coil holders cannot compensate any movements of the subject (Hynninen and Järnefelt 2015).

---

<sup>20</sup> The physics of the magnetic and electrical stimulation fields is linear so that the problem can, for example, be solved for gyrus-precise anatomy models through mathematical convolution of the anatomy with a Green's function of a specific coil, which is computationally notably faster than solving strongly coupled equation systems derived from the Maxwell equations in real time.

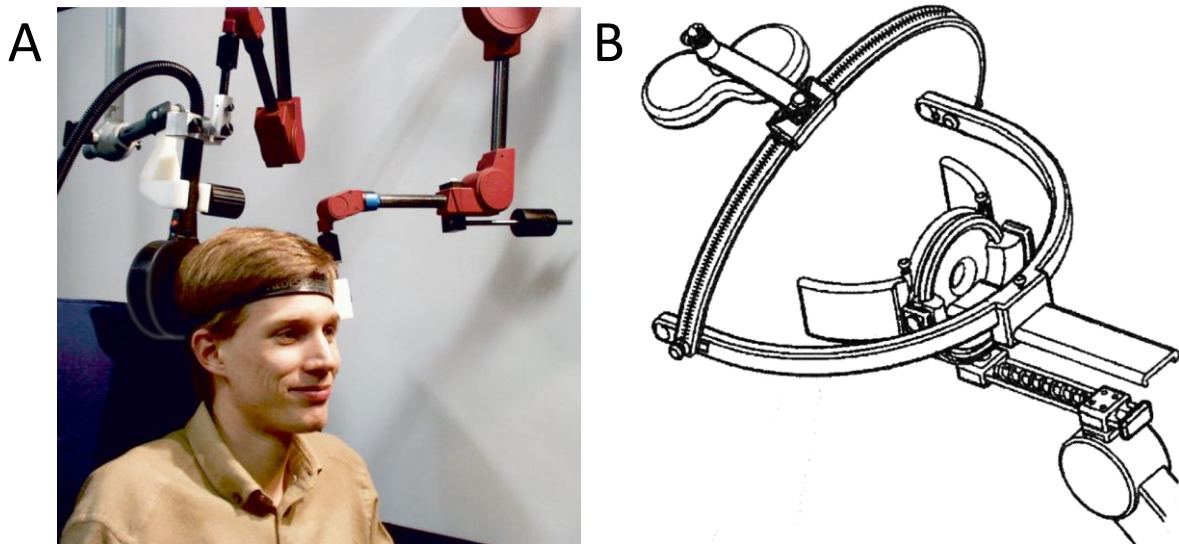


**Figure 7.7 about here**

**Caption:** A. Mechanical coil holder for TMS with stereotactical position read-out of the stimulation transducer through calibrated goniometers at each joint from around 1996 based on a commercial position digitization system of the time (specifically MicroScribe 3DX, Immersion Corporation, San Jose (CA), USA) and used in various TMS studies (Kammer, Beck, Thielscher, et al. 2001). B. Commercially available mechanical holder with spherical kinematics adjusted for brain stimulation reminding of stereotactic frames from surgery and following earlier designs from the 1990s (Traad 1990; Wölfel, Hirschbeck, and Häringer 2018; Cameron et al. 2010) (Courtesy of Mag&More, Munich, Germany).

Brain stimulation during walking or other exercises often uses dedicated transducer holders that deal with the motion as well as associated forces and typically either mount or fix the transducer on a helmet-like setup or lock the head position relative to the torso (Schubert et al. 1997; Taube et al. 2008; Barthélemy et al. 2012). Similar solutions have recently been suggested to individualize coil positioning for medical treatment through custom-made rigs or helmets based on individual imaging data, and commercialization has been announced (Mansouri et al. 2018).

For a well-defined head position (e.g., with a head rest that enforces a certain head posture), the required action space is typically smaller and frames with finer adjustment means can allow millimeter- and degree-level tuning of position and orientation, respectively (Traad 1990; Wölfel, Hirschbeck, and Häringer 2018; Cameron et al. 2010). Those conditions are typically met in imaging scanners, for which sophisticated nonmagnetic setups are available (Moisa et al. 2009; Bohning et al. 2003). If such high-accuracy setups are combined with conventional general-purpose arms, they tend to suffer from the mechanical tolerances of the latter. Furthermore, subjects with either freely moving or constrained heads tend to constantly move (e.g., due to muscle contraction), which can worsen if subjects visually scan the room, have to follow a moving object on a screen in a task, or have certain medical conditions (Fuller 1992; Stahl 1999; Goetz et al. 2018; Treleven 2008). Even small movements of the transducer relative to the brain practically reduce the precision of stimulation in neuromodulation interventions and increase the endogenous trial-to-trial variability of the response to brain stimulation (Ellaway et al. 1998; Amassian, Cracco, and Maccabee 1989; Goetz et al. 2014). Vacuum pillows adopted from traumatology are sometimes used to stabilize the head position, but reports on the accuracy of this approach are lacking (Topp and Patten 2015).

## Robotic transducer positioning

Navigated robotic systems promise improvements in positioning as they can reach a location with high accuracy and compensate movements of the subject (Richter, Neumann, et al. 2013; Lancaster et al. 2004; Kantelhardt et al. 2010; Lebosse et al. 2007; Richter, Bruder, et al. 2010; Zorn et al. 2012; Richter, Trillenber, et al. 2013). These systems currently focus on TMS but could, in principle, serve for ultrasound stimulation as well. The majority of setups use articulated robots with series kinematics, as shown in Figure 7.8, which are commonly used for assembly-line welding (Richter, Bruder, et al. 2010; Lancaster et al. 2004). Although the sub-millimeter accuracy of industrial robots is sufficient, custom kinematics can align the main axes of the robot with those of the human head and, in principle, achieve a wider action space with an overall smaller setup.<sup>21</sup> This adjustment can increase repositioning speed in the most relevant directions, avoid singularities requiring compensation movements of the articulations, and add safety features (Lebosse et al. 2007; Zorn et al. 2012; Shiakolas, Conrad, and Yih 2002).



**Figure 7.8** about here

**Caption:** Robotic targeting setup with an industrial robot, which tracks the head position through a stereo camera and infrared reflectors on the head.

More important than the kinematics might be the control. Most available systems are combined with stereotaxy to track the position of the subject's head (Richter, Bruder, et al. 2010; Richter, Matthäus, et al. 2010). Some of those further use position control so that their control loop minimizes the distance of the transducer to the set position and orientation (Lebosse et al. 2007; Richter, Bruder, et

---

<sup>21</sup> Such alignment was already suggested for the first passive coil holders (Traad 1990).

al. 2010). However, position control alone suffers from limitations, such as a challenge in establishing a stable, well-defined contact between the stimulation transducer and the head, which is relevant for both TMS and ultrasound stimulation. A well-defined contact with some friction helps to reduce the oscillatory and random-walk-like movements that subjects perform trying to stabilize their head, and also avoids painful pressure of the transducer on the head. With position control only, subjects tend either to lean against the transducer if the contact is loose, with the effect of systematically pushing it further away into that direction, or to feel pushed by the transducer and move away, while the robot keeps following (Goetz et al. 2018; Goetz et al. 2016). As this process is subtle, the drift can be as slow as a millimeter per second or less, but generally leads to leaving the robot action space and/or forcing the subject into an uncomfortable posture. Since neither the transducer nor the head are particularly elastic, even sub-millimeter deviations from the set position of the transducer can cause either too loose or too tight contact. In ultrasound stimulation, direct mechanical or gel-mediated contact is further required to transmit the sound to the skull (Wattiez et al. 2017; Tufail et al. 2010; Tufail et al. 2011). For safety, robot controllers limit the speed of the effector and all joints to minimize the momentum in case of a collision (Richter and Bruder 2013). Typical speeds are below 10 mm/s, which leads to so-called slewing if subjects move faster (Kantelhardt et al. 2010; Zorn et al. 2012; Richter 2013).

In robotic setups, subjects can typically move their head relatively freely but are encouraged to keep their head as still as possible and move only slowly so that the robot can follow (Ginhoux et al. 2013; Kantelhardt et al. 2010; Goetz et al. 2018). Head rests in combination with exclusive position control can be critical because the robot is physically strong enough to harm the subject, e.g., if it pushes the head against any fixed object. Most industrial robots have a torque and collision detection, often based on the current of its motors in the joints to trigger an emergency shut off; alternatively, torque or force sensors can be used (Richter and Bruder 2013). However, in either case, a detected collision usually shuts off the system completely, terminates a session and may lead to loss of the session configuration. In addition to position control, the robot can control the head–transducer contact, e.g., the normal force (Lebosse et al. 2011; Zorn et al. 2012). In a workaround, an elastic element introduced between the transducer and the head can enhance pure position control of a robot (Goetz et al. 2018). The elasticity links transducer–head distance and force or pressure so that the otherwise exclusive position control loop receives a pressure control component. The elastic element may be detrimental for ultrasound stimulation but acceptable for TMS if it is sufficiently thin to avoid the need for substantially higher machine output for the same field strength at the target and any considerable loss of focality due to the increased distance (McConnell et al. 2001; Thielscher and Kammer 2004; Goetz and Deng 2017; Hewitt, Meincke, and Liebetanz 2017).

Available robotic setups offer several modes. Typically, the robot can run a motion-compensation mode, where it keeps the latest position and orientation of the stimulation transducer constant relative to the subject's head, which could be manually set up beforehand. Alternatively, the robotic system can bring the transducer to a specified head-referenced position, such as in Talairach or MNI coordinates, or scan a number of points successively, for instance, for cortical mapping (Finke et al. 2008; Kantelhardt et al. 2010; Meincke et al. 2016; Meincke et al. 2018). However, as in conventional neuronavigation, establishing the relationship between the placement of the transducer and the actual target in the brain requires a model of the physics and physiology of the specific stimulation technology and is usually not part of available robot systems. Finally, cooperative systems—inspired by research in human–robot interaction and often abbreviated as cobots—allow the operator to interact with the robot more immediately and intuitively (Dimeas and Aspragathos 2016; Lee et al. 2014; Richter, Bruder, and Schweikard 2012). Instead of only setting positions through software, e.g., a module in the neuronavigation user interface, operators can, for instance, move the stimulation transducer manually while the robot compensates a majority of the forces, such as the robot's and

transducer's weight. Manual coil repositioning with a cobot can simplify and accelerate a hotspot search or comparable dynamic procedures with frequent transducer movements for experienced operators, particularly as fully automated methods are still time-consuming mostly due to still slow robotic repositioning. Similarly, the more immediate interaction with a cobot allows manual readjustment of positioning errors or rapid movements more convenient and faster than actuation through a mouse or keyboard interface.

Reported positioning accuracies throughout a procedure range from less than one millimeter (Lancaster et al. 2004) to a few millimeters (Zorn et al. 2012), with the robotic systems typically outperforming manual holding by at least 40% lower positioning error in direct comparison (Ginhoux et al. 2013). In actual studies with human subjects, such low errors relative to the initially set position appear achievable but tend to slowly grow throughout the session (Goetz et al. 2018). Moreover, robotic positioning with stereotaxy inherits the general limitations of neuronavigation, such as tracker sliding due to unreliable headband mounting.

For studies with robotic actuator positioning, sufficient time for setting up each subject has to be budgeted in, which was reported to be approximately 14 min for one commercial system (Goetz et al. 2018). Improved solutions might reduce such set-up time and enable the use in clinical applications for a higher degree of automation and reproducibility.

### Acknowledgements

The authors thank Daniela De Albuquerque, Dr. J. Matias Di Martino, Alexander Shang, and Raymond Lin for reading the chapter and providing helpful suggestions.

## References

- Ahdab, R., S. S. Ayache, P. Brugières, C. Goujon, and J. P. Lefaucheur. 2010. 'Comparison of "standard" and "navigated" procedures of TMS coil positioning over motor, premotor and prefrontal targets in patients with chronic pain and depression', *Neurophysiologie Clinique/Clinical Neurophysiology*, 40: 27-36.
- Alam, Mahtab, Dennis Q. Truong, Niranjan Khadka, and Marom Bikson. 2016. 'Spatial and polarity precision of concentric high-definition transcranial direct current stimulation (HD-tDCS)', *Physics in Medicine and Biology*, 61: 4506-4521.
- Amassian, Vahe E., Roger Q. Cracco, and Paul J. Maccabee. 1989. 'Focal stimulation of human cerebral cortex with the magnetic coil: a comparison with electrical stimulation', *Electroencephalography and Clinical Neurophysiology/Evoked Potentials Section*, 74: 401-416.
- Amassian, Vahe E., Roger Q. Cracco, Paul J. Maccabee, Joan B. Cracco, Alan Rudell, and Larry Eberle. 1989. 'Suppression of visual perception by magnetic coil stimulation of human occipital cortex', *Electroencephalography and Clinical Neurophysiology/Evoked Potentials Section*, 74: 458-462.
- Amassian, Vahe, Zoltan Mari, Laura Saggiocco, Nasser Hassan, Peter Maccabee, Joan B. Cracco, Roger Q. Cracco, and Ivan Bodis-Wollner. 2008. 'Perception of Phosphenes and Flashed Alphabetical Characters is Enhanced by Single-Pulse Transcranial Magnetic Stimulation of Anterior Frontal Lobe: The Thalamic Gate Hypothesis', *Perception*, 37: 375-388.
- Ambrosini, Emilia, Simona Ferrante, Mark van de Ruit, Stefano Biguzzi, Vera Colombo, Marco Monticone, Giorgio Ferriero, Alessandra Pedrocchi, Giancarlo Ferrigno, and Michael J. Grey. 2018. 'StimTrack: An open-source software for manual transcranial magnetic stimulation coil positioning', *Journal of Neuroscience Methods*, 293: 97-104.
- Andoh, Jamila, Denis Riviere, Jean-François Mangin, Eric Artiges, Yann Cointepas, David Grevent, Marie-Laure Paillère-Martinot, Jean-Luc Martinot, and Arnaud Cachia. 2009. 'A triangulation-based magnetic resonance image-guided method for transcranial magnetic stimulation coil positioning', *Brain Stimulation*, 2: 123-131.
- Antonenko, Daria, Axel Thielscher, Guilherme Bicalho Saturnino, Semiha Aydin, Bernd Ittermann, Ulrike Grittner, and Agnes Flöel. 2019. 'Towards precise brain stimulation: Is electric field simulation related to neuromodulation?', *Brain Stimulation*, 12: 1159-1168.
- Aonuma, Shinta, Jose Gomez-Tames, Ilkka Laakso, Akimasa Hirata, Tomokazu Takakura, Manabu Tamura, and Yoshihiro Muragaki. 2018. 'A high-resolution computational localization method for transcranial magnetic stimulation mapping', *NeuroImage*, 172: 85-93.
- Barnett, G. H., D. W. Kormos, C. P. Steiner, and H. Morris. 1993. 'Registration of EEG Electrodes with Three-Dimensional Neuroimaging Using a Frameless, Armless Stereotactic Wand', *Stereotactic and Functional Neurosurgery*, 61: 32-38.
- Barthélemy, D., S. Alain, M. J. Grey, J. B. Nielsen, and L. J. Bouyer. 2012. 'Rapid changes in corticospinal excitability during force field adaptation of human walking', *Experimental Brain Research*, 217: 99-115.
- Bastings, Eric P., H. Donald Gage, Jason P. Greenberg, Greg Hammond, Luis Hernandez, Peter Santago, Craig A. Hamilton, Dixon M. Moody, Krish D. Singh, Peter E. Ricci, Tim P. Pons, and David Good. 1998. 'Co-registration of cortical magnetic stimulation and functional magnetic resonance imaging', *NeuroReport*, 9: 1941-1946.
- Beisteiner, Roland, Eva Matt, Christina Fan, Heike Baldysiak, Marleen Schönfeld, Tabea Philippi Novak, Ahmad Amini, Tuna Aslan, Raphael Reinecke, Johann Lehrner, Alexandra Weber, Ulrike Reime, Cédric Goldenstedt, Ernst Marlinghaus, Mark Hallett, and Henning Lohse-Busch. 2020. 'Transcranial Pulse Stimulation with Ultrasound in Alzheimer's Disease—A New Navigated Focal Brain Therapy', *Advanced Science*, 7: 1902583.
- Benjemaa, Raouf, and Francis Schmitt. 1998. "A solution for the registration of multiple 3D point sets using unit quaternions." In *Computer Vision — ECCV'98*, edited by Hans Burkhardt and Bernd Neumann, 34-50. Berlin, Heidelberg: Springer.

- Benligiray, Burak, Cihan Topal, and Cuneyt Akinlar. 2019. 'STag: A stable fiducial marker system', *Image and Vision Computing*, 89: 158-169.
- Bijsterbosch, Janine D., Anthony T. Barker, Kwang-Hyuk Lee, and P. W. R. Woodruff. 2012. 'Where does transcranial magnetic stimulation (TMS) stimulate? Modelling of induced field maps for some common cortical and cerebellar targets', *Medical & Biological Engineering & Computing*, 50: 671-681.
- Bikson, M., Abhishek Datta, Fortunato Battaglia, and Maged Elwassif. 2014. 'Apparatus and method for neurocranial electrostimulation', Research Foundation of the City University of New York, Patent US 8,718,778, US 61/124,286, U.S. Patent and Trademark Office.
- Bikson, Marom, Asif Rahman, and Abhishek Datta. 2012. 'Computational Models of Transcranial Direct Current Stimulation', *Clinical EEG and Neuroscience*, 43: 176-183.
- Bohning, Daryl E., S. Denslow, P. A. Bohning, J. A. Walker, and M. S. George. 2003. 'A TMS coil positioning/holding system for MR image-guided TMS interleaved with fMRI', *Clinical Neurophysiology*, 114: 2210-2219.
- Brasil-Neto, Joaquim P., Leonardo G. Cohen, Marcela Panizza, Jan Nilsson, Bradley J. Roth, and Mark Hallett. 1992. 'Optimal Focal Transcranial Magnetic Activation of the Human Motor Cortex: Effects of Coil Orientation, Shape of the Induced Current Pulse, and Stimulus Intensity', *Journal of Clinical Neurophysiology*, 9: 132-136.
- Brodmann, Korbinian. 1909. *Vergleichende Lokalisationslehre der Großhirnrinde, in ihren Prinzipien dargestellt auf Grund des Zellenbaues* (Verlag Johann Ambrosius Barth: Leipzig).
- Bungert, Andreas, André Antunes, Svenja Espenhahn, and Axel Thielscher. 2017. 'Where does TMS Stimulate the Motor Cortex? Combining Electrophysiological Measurements and Realistic Field Estimates to Reveal the Affected Cortex Position', *Cerebral Cortex*, 27: 5083-5094.
- Cameron, Allan, John A. McNeill, Gregg Flender, and Mark Edward Riehl. 2010. 'Method and apparatus for coil positioning for TMS studies', Neuronetics Inc., Patent US 7,651,459, US 10/752,164, U.S. Patent and Trademark Office.
- Cash, Robin F. H., Luca Cocchi, Jinglei Lv, Yumeng Wu, Paul B. Fitzgerald, and Andrew Zalesky. 2021. 'Personalized connectivity-guided DLPFC-TMS for depression: Advancing computational feasibility, precision and reproducibility', *Human Brain Mapping*, 42: 4155-4172.
- Cash, Robin F. H., Anne Weigand, Andrew Zalesky, Shan H. Siddiqi, Jonathan Downar, Paul B. Fitzgerald, and Michael D. Fox. 2020. 'Using Brain Imaging to Improve Spatial Targeting of Transcranial Magnetic Stimulation for Depression', *Biological Psychiatry*, in press.
- Cash, Robin F. H., Andrew Zalesky, Richard H. Thomson, Ye Tian, Luca Cocchi, and Paul B. Fitzgerald. 2019. 'Subgenual Functional Connectivity Predicts Antidepressant Treatment Response to Transcranial Magnetic Stimulation: Independent Validation and Evaluation of Personalization', *Biological Psychiatry*, 86(2): e5-e7.
- Chou, J. C. K. 1992. 'Quaternion kinematic and dynamic differential equations', *IEEE Transactions on Robotics and Automation*, 8: 53-64.
- Chronicle, Edward P., A. Jane Pearson, and Cheryl Matthews. 2005. 'Development and Positioning Reliability of a TMS Coil Holder for Headache Research', *Headache: The Journal of Head and Face Pain*, 45: 37-41.
- Clarke, J. V., A. H. Deakin, A. C. Nicol, and F. Picard. 2010. 'Measuring the positional accuracy of computer assisted surgical tracking systems', *Computer Aided Surgery*, 15: 13-18.
- Clement, G. T., and K. Hynynen. 2002. 'A non-invasive method for focusing ultrasound through the human skull', *Physics in Medicine & Biology*, 47: 1219.
- Cole, Eleanor J., Katy H. Stimpson, Brandon S. Bentzley, Merve Gulser, Kirsten Cherian, Claudia Tischler, Romina Nejad, Heather Pankow, Elizabeth Choi, Haley Aaron, Flint M. Espil, Jaspreet Pannu, Xiaoqian Xiao, Dalton Duvio, Hugh B. Solvason, Jessica Hawkins, Austin Guerra, Booil Jo, Kristin S. Raj, Angela L. Phillips, Fahim Barmak, James H. Bishop, John P. Coetzee, Charles DeBattista, Jennifer Keller, Alan F. Schatzberg, Keith D. Sudheimer, and Nolan R. Williams. 2020. 'Stanford Accelerated Intelligent Neuromodulation Therapy for Treatment-Resistant Depression', *American Journal of Psychiatry*, 177: 716-726.

- D'Ostilio, Kevin, Stefan M. Goetz, Ricci Hannah, Matteo Ciocca, Raffaella Chieffo, Jui-Cheng A. Chen, Angel V. Peterchev, and John C. Rothwell. 2016. 'Effect of coil orientation on strength–duration time constant and I-wave activation with controllable pulse parameter transcranial magnetic stimulation', *Clinical Neurophysiology*, 127: 675-683.
- Dai, H., Y. Zeng, Z. Wang, H. Lin, M. Lin, H. Gao, S. Song, and M. Q. H. Meng. 2020. 'Prior Knowledge-Based Optimization Method for the Reconstruction Model of Multicamera Optical Tracking System', *IEEE Transactions on Automation Science and Engineering*, 17: 2074-2084.
- Dannhauer, Moritz, Ziping Huang, Lysianne Beynel, Eleanor Wood, Noreen Bukhari-Parlakturk, and Angel V. Peterchev. 2021. 'Targeting and analysis pipeline for optimization and verification of TMS coil placement', *bioRxiv*: 2021.05.09.443339.
- Datta, Abhishek. 2020. Neural Navigator. Soterix Stereotaxic Neuronavigation System. Food and Drug Administration, U.S. Department of Health & Human Services, K191422.
- Datta, Abhishek, Varun Bansal, Julian Diaz, Jinal Patel, Davide Reato, and Marom Bikson. 2009. 'Gyri-precise head model of transcranial direct current stimulation: Improved spatial focality using a ring electrode versus conventional rectangular pad', *Brain Stimulation*, 2: 201-207.e1.
- De Witte, Sara, Debby Klooster, Josefien Dedoncker, Romain Duprat, Jonathan Remue, and Chris Baeken. 2018. 'Left prefrontal neuronavigated electrode localization in tDCS: 10–20 EEG system versus MRI-guided neuronavigation', *Psychiatry Research: Neuroimaging*, 274: 1-6.
- Deng, Zhi-De, Sarah H. Lisanby, and Angel V. Peterchev. 2013. 'Electric field depth–focality tradeoff in transcranial magnetic stimulation: Simulation comparison of 50 coil designs', *Brain Stimulation*, 6: 1-13.
- Devlin, Joseph T., and Kate E. Watkins. 2007. 'Stimulating language: insights from TMS', *Brain*, 130: 610-622.
- Dimeas, F., and N. Aspragathos. 2016. 'Online Stability in Human-Robot Cooperation with Admittance Control', *IEEE Transactions on Haptics*, 9: 267-278.
- Dmochowski, Jacek P. , Abhishek Datta, Marom Bikson, Yuzhuo Su, and Lucas C. Parra. 2011. 'Optimized multi-electrode stimulation increases focality and intensity at target', *Journal of Neural Engineering*, 8: 046011.
- Edwards, Dylan, Mar Cortes, Abhishek Datta, Preet Minhas, Eric M. Wassermann, and Marom Bikson. 2013. 'Physiological and modeling evidence for focal transcranial electrical brain stimulation in humans: A basis for high-definition tDCS', *NeuroImage*, 74: 266-275.
- Elfring, Robert, Matías de la Fuente, and Klaus Radermacher. 2010. 'Assessment of optical localizer accuracy for computer aided surgery systems', *Computer Aided Surgery*, 15: 1-12.
- Ellaway, P. H., N. J. Davey, D. W. Maskill, S. R. Rawlinson, H. S. Lewis, and N. P. Anissimova. 1998. 'Variability in the amplitude of skeletal muscle responses to magnetic stimulation of the motor cortex in man', *Electroencephalography and Clinical Neurophysiology/Electromyography and Motor Control*, 109: 104-113.
- Epstein, Charles M., and Kent R. Davey. 2002. 'Iron-Core Coils for Transcranial Magnetic Stimulation', *Journal of Clinical Neurophysiology*, 19: 376-381.
- Esterman, Michael, Michelle Thai, Hidefusa Okabe, Joseph DeGutis, Elyana Saad, Simon E. Laganieri, and Mark A. Halko. 2017. 'Network-targeted cerebellar transcranial magnetic stimulation improves attentional control', *NeuroImage*, 156: 190-198.
- Ettinger, G. J., M. E. Leventon, W. E. L. Grimson, R. Kikinis, L. D. Gugino, W. Cote, L. Sprung, L. Aglio, M. E. Shenton, G. Potts, V. L. Hernandez, and E. Alexander. 1998. 'Experimentation with a transcranial magnetic stimulation system for functional brain mapping', *Medical Image Analysis*, 2: 133-142.
- Finke, M., T. Fadini, S. Kantelhardt, A. Giese, L. Matthaus, and A. Schweikard. 2008. 'Brain-mapping using robotized TMS', *IEEE Proc. Eng. Med. Biol.*, 30: 3929-3932.
- Fischer, D. B., P. J. Fried, G. Ruffini, O. Ripolles, R. Salvador, J. Banus, W. T. Ketchabaw, E. Santarnecchi, A. Pascual-Leone, and M. D. Fox. 2017. 'Multifocal tDCS targeting the resting state motor network increases cortical excitability beyond traditional tDCS targeting unilateral motor cortex', *NeuroImage*, 157: 34-44.

- Fitzgerald, Paul B. 2021. 'Targeting repetitive transcranial magnetic stimulation in depression: do we really know what we are stimulating and how best to do it?', *Brain Stimulation*, 14: 730-736.
- Fitzgerald, Paul B., Kate Hoy, Susan McQueen, Jerome J. Maller, Sally Herring, Rebecca Segrave, Michael Bailey, Greg Been, Jayashri Kulkarni, and Zafiris J. Daskalakis. 2009. 'A Randomized Trial of rTMS Targeted with MRI Based Neuro-Navigation in Treatment-Resistant Depression', *Neuropsychopharmacology*, 34: 1255.
- Fox, Michael D., Randy L. Buckner, Matthew P. White, Michael D. Greicius, and Alvaro Pascual-Leone. 2012. 'Efficacy of Transcranial Magnetic Stimulation Targets for Depression Is Related to Intrinsic Functional Connectivity with the Subgenual Cingulate', *Biological Psychiatry*, 72: 595-603.
- Fox, Michael D., Hesheng Liu, and Alvaro Pascual-Leone. 2013. 'Identification of reproducible individualized targets for treatment of depression with TMS based on intrinsic connectivity', *NeuroImage*, 66: 151-160.
- Frantz, D. D., A. D. Wiles, S. E. Leis, and S. R. Kirsch. 2003. 'Accuracy assessment protocols for electromagnetic tracking systems', *Physics in Medicine and Biology*, 48: 2241-2251.
- Franz, A. M., T. Haidegger, W. Birkfellner, K. Cleary, T. M. Peters, and L. Maier-Hein. 2014. 'Electromagnetic Tracking in Medicine—A Review of Technology, Validation, and Applications', *IEEE Transactions on Medical Imaging*, 33: 1702-1725.
- Fuller, James H. 1992. 'Head movement propensity', *Experimental Brain Research*, 92: 152-164.
- George, Mark S., Sarah H. Lisanby, David Avery, William M. McDonald, Valerie Durkalski, Martina Pavlicova, Berry Anderson, Ziad Nahas, Peter Bulow, Paul Zarkowski, Paul E. Holtzheimer, III, Theresa Schwartz, and Harold A. Sackeim. 2010. 'Daily Left Prefrontal Transcranial Magnetic Stimulation Therapy for Major Depressive Disorder: A Sham-Controlled Randomized Trial', *Archives of General Psychiatry*, 67: 507-516.
- George, Mark S., Eric M. Wassermann, Tim A. Kimbrell, John T. Little, Wendol E. Williams, Aimee L. Danielson, Benjamin D. Greenberg, Mark Hallett, and Robert M. Post. 1997. 'Mood Improvement Following Daily Left Prefrontal Repetitive Transcranial Magnetic Stimulation in Patients With Depression: A Placebo-Controlled Crossover Trial', *American Journal of Psychiatry*, 154: 1752-1756.
- Gerschlagner, Willibald, Hartwig R. Siebner, and John C. Rothwell. 2001. 'Decreased corticospinal excitability after subthreshold 1 Hz rTMS over lateral premotor cortex', *Neurology*, 57: 449-455.
- Gershon, Ari A., Pinhas N. Dannon, and Leon Grunhaus. 2003. 'Transcranial Magnetic Stimulation in the Treatment of Depression', *American Journal of Psychiatry*, 160: 835-845.
- Ginhoux, R., P. Renaud, L. Zorn, L. Goffin, B. Bayle, J. Foucher, J. Lamy, J. P. Armspach, and M. de Mathelin. 2013. "A custom robot for Transcranial Magnetic Stimulation: First assessment on healthy subjects." In *2013 35th Annual International Conference of the IEEE Engineering in Medicine and Biology Society (EMBC)*, 5352-5355.
- Goetz, S. M., I. Cassie Kozyrkov, Bruce Luber, S. H. Lisanby, D. L. K. Murphy, Warren M. Grill, and A. V. Peterchev. 2018. 'Accuracy of robotic coil positioning during transcranial magnetic stimulation', *Journal of Neural Engineering*, 16(5): 054003.
- Goetz, Stefan M., and Zhi-De Deng. 2017. 'The development and modelling of devices and paradigms for transcranial magnetic stimulation', *International Review of Psychiatry*, 29: 115-145.
- Goetz, Stefan M., Bruce Luber, Sarah H. Lisanby, David L. K. Murphy, I. Cassie Kozyrkov, Warren M. Grill, and Angel V. Peterchev. 2016. 'Enhancement of Neuromodulation with Novel Pulse Shapes Generated by Controllable Pulse Parameter Transcranial Magnetic Stimulation', *Brain Stimulation*, 9: 39-47.
- Goetz, Stefan M., Bruce Luber, Sarah H. Lisanby, and Angel V. Peterchev. 2014. 'A Novel Model Incorporating Two Variability Sources for Describing Motor Evoked Potentials', *Brain Stimulation*, 7: 541-552.
- Goldman, Ron. 2011. 'Understanding quaternions', *Graphical Models*, 73: 21-49.

- Golfinos, John G., Brian C. Fitzpatrick, Lawrence R. Smith, and Robert F. Spetzler. 1995. 'Clinical use of a frameless stereotactic arm: results of 325 cases', *Journal of Neurosurgery*, 83: 197-205.
- Gomez-Tames, Jose, Atsushi Hamasaka, Ilkka Laakso, Akimasa Hirata, and Yoshikazu Ugawa. 2018. 'Atlas of optimal coil orientation and position for TMS: A computational study', *Brain Stimulation*, 11: 839-848.
- Gomez, Luis J., Moritz Dannhauer, and Angel V. Peterchev. 2021. 'Fast computational optimization of TMS coil placement for individualized electric field targeting', *NeuroImage*, 228: 117696.
- Goodwin, Brian D., and Christopher R. Butson. 2015. 'Subject-Specific Multiscale Modeling to Investigate Effects of Transcranial Magnetic Stimulation', *Neuromodulation: Technology at the Neural Interface*, 18: 694-704.
- Groppa, Sergiu, Boris H. Schlaak, Alexander Münchau, Nicole Werner-Petroll, Janin Dünneweber, Tobias Bäumer, Bart F.L. van Nuenen, and Hartwig R. Siebner. 2012. 'The human dorsal premotor cortex facilitates the excitability of ipsilateral primary motor cortex via a short latency cortico-cortical route', *Human Brain Mapping*, 33: 419-430.
- Gugino, Laverne D., J. Rafael Romero, Linda Aglio, Debra Titone, Marcela Ramirez, Alvaro Pascual-Leone, Eric Grimson, Neil Weisenfeld, Ron Kikinis, and Martha- E. Shenton. 2001. 'Transcranial magnetic stimulation coregistered with MRI: a comparison of a guided versus blind stimulation technique and its effect on evoked compound muscle action potentials', *Clinical Neurophysiology*, 112: 1781-1792.
- Halawa, I., Y. Shirota, A. Neef, M. Sommer, and W. Paulus. 2019. 'Neuronal tuning: Selective targeting of neuronal populations via manipulation of pulse width and directionality', *Brain Stimulation*, 12: 399.
- Hamilton, William Rowan. 1844-1850. 'On Quaternions; or on a new System of Imaginaries in Algebra', *The London, Edinburgh and Dublin Philosophical Magazine and Journal of Science*, XXV-XXXVI.
- Hannula, Henri, Tuomas Neuvonen, Petri Savolainen, Jaana Hiltunen, Yuan-Ye Ma, Hanne Antila, Oili Salonen, Synnöve Carlson, and Antti Pertovaara. 2010. 'Increasing top-down suppression from prefrontal cortex facilitates tactile working memory', *NeuroImage*, 49: 1091-1098.
- Hannula, Henri, Shelley Ylloja, Antti Pertovaara, Antti Korvenoja, Jarmo Ruohonen, Risto J. Ilmoniemi, and Synnöve Carlson. 2005. 'Somatotopic blocking of sensation with navigated transcranial magnetic stimulation of the primary somatosensory cortex', *Human Brain Mapping*, 26: 100-109.
- Hartley, Richard I., and Peter Sturm. 1997. 'Triangulation', *Computer Vision and Image Understanding*, 68: 146-157.
- Herbsman, Tal, David Avery, Dave Ramsey, Paul Holtzheimer, Chandra Wadjik, Frances Hardaway, David Haynor, Mark S. George, and Ziad Nahas. 2009. 'More Lateral and Anterior Prefrontal Coil Location Is Associated with Better Repetitive Transcranial Magnetic Stimulation Antidepressant Response', *Biological Psychiatry*, 66: 509-515.
- Herwig, Uwe, Peyman Satrapi, and Carlos Schönfeldt-Lecuona. 2003. 'Using the International 10-20 EEG System for Positioning of Transcranial Magnetic Stimulation', *Brain Topography*, 16: 95-99.
- Hewitt, M., J. Meincke, and D. Liebetanz. 2017. 'P161 Robot-guided approach to the correlation of TMS intensity and focality in man', *Clinical Neurophysiology*, 128: e96.
- Hironaga, Naruhito, Takahiro Kimura, Takako Mitsudo, Atsuko Gunji, and Makoto Iwata. 2018. 'Proposal for an accurate TMS-MRI co-registration process via 3D laser scanning', *Neuroscience Research*, 144: 30-39.
- Höflich, G., S. Kasper, A. Hufnagel, S. Ruhmann, and H. J. Möller. 1993. 'Application of transcranial magnetic stimulation in treatment of drug-resistant major depression—a report of two cases', *Human Psychopharmacology: Clinical and Experimental*, 8: 361-365.
- Hynninen, Pentti, and Gustav Järnefelt. 2015. 'Device support apparatus', Nexstim Oy, Patent US 10,188,868, US 2015/0151137, US 14/093,073, U.S. Patent and Trademark Office.

- Iseger, Tabitha A., Frank Padberg, J. Leon Kenemans, Richard Gevirtz, and Martijn Arns. 2017. 'Neuro-Cardiac-Guided TMS (NCG-TMS): Probing DLPFC-sgACC-vagus nerve connectivity using heart rate – First results', *Brain Stimulation*, 10: 1006-1008.
- Iseger, Tabitha A., Nienke E. R. van Bueren, J. Leon Kenemans, Richard Gevirtz, and Martijn Arns. 2020. 'A frontal-vagal network theory for Major Depressive Disorder: Implications for optimizing neuromodulation techniques', *Brain Stimulation*, 13: 1-9.
- Jaroonsorn, Prakarn, Paramin Neranon, Pruittikorn Smithmaitrie, and Charoenyut Dechwayukul. 2020. 'Implementation of an autonomous assistive robotic system for transcranial magnetic stimulation', *Journal of Mechanical Engineering*, 43: 308-320.
- Jasper, Herbert H. 1958. 'Report of the committee on methods of clinical examination in electroencephalography', *Electroencephalography and Clinical Neurophysiology*, 10: 370-375.
- Jeltema, Hanne-Rinck, Ann-Katrin Ohlerth, Aranka de Wit, Michiel Wagemakers, Adrià Rofes, Roelien Bastiaanse, and Gea Drost. 2021. 'Comparing navigated transcranial magnetic stimulation mapping and “gold standard” direct cortical stimulation mapping in neurosurgery: a systematic review', *Neurosurgical Review*, 44: 1903-1920.
- Julkunen, Petro. 2014. 'Methods for estimating cortical motor representation size and location in navigated transcranial magnetic stimulation', *Journal of Neuroscience Methods*, 232: 125-133.
- Julkunen, Petro, Laura Säisänen, Nils Danner, Eini Niskanen, Taina Hukkanen, Esa Mervaala, and Mervi Könönen. 2009. 'Comparison of navigated and non-navigated transcranial magnetic stimulation for motor cortex mapping, motor threshold and motor evoked potentials', *NeuroImage*, 44: 790-795.
- Jung, Nikolai H., Igor Delvendahl, Nicola G. Kuhnke, Dieter Hauschke, Sabine Stolle, and Volker Mall. 2010. 'Navigated transcranial magnetic stimulation does not decrease the variability of motor-evoked potentials', *Brain Stimulation*, 3: 87-94.
- Kammer, Thomas, Sandra Beck, Michael Erb, and Wolfgang Grodd. 2001. 'The influence of current direction on phosphene thresholds evoked by transcranial magnetic stimulation', *Clinical Neurophysiology*, 112: 2015-2021.
- Kammer, Thomas, Sandra Beck, Axel Thielscher, Ulrike Laubis-Herrmann, and Helge Topka. 2001. 'Motor thresholds in humans: a transcranial magnetic stimulation study comparing different pulse waveforms, current directions and stimulator types', *Clinical Neurophysiology*, 112: 250-258.
- Kammer, Thomas, Klaas Puls, Michael Erb, and Wolfgang Grodd. 2005. 'Transcranial magnetic stimulation in the visual system. II. Characterization of induced phosphenes and scotomas', *Experimental Brain Research*, 160: 129-140.
- Kammer, Thomas, Michael Vorweg, and Bärbel Herrnberger. 2007. 'Anisotropy in the visual cortex investigated by neuronavigated transcranial magnetic stimulation', *NeuroImage*, 36: 313-221.
- Kanda, Masutaro, Tatsuya Mima, Tatsuhide Oga, Masao Matsushashi, Keiichiro Toma, Hidemi Hara, Takeshi Satow, Takashi Nagamine, John C. Rothwell, and Hiroshi Shibasaki. 2003. 'Transcranial magnetic stimulation (TMS) of the sensorimotor cortex and medial frontal cortex modifies human pain perception', *Clinical Neurophysiology*, 114: 860-866.
- Kantelhardt, Sven Rainer, Tommaso Fadini, Markus Finke, Kai Kallenberg, Jakob Siemerikus, Volker Bockermann, Lars Matthaeus, Walter Paulus, Achim Schweikard, Veit Rohde, and Alf Giese. 2010. 'Robot-assisted image-guided transcranial magnetic stimulation for somatotopic mapping of the motor cortex: a clinical pilot study', *Acta Neurochirurgica*, 152: 333-343.
- Kaur, Manreena, Jessica A. Michael, Kate E. Hoy, Bernadette M. Fitzgibbon, Megan S. Ross, Tabitha A. Iseger, Martijn Arns, Abdul-Rahman Hudaib, and Paul B. Fitzgerald. 2020. 'Investigating high- and low-frequency neuro-cardiac-guided TMS for probing the frontal vagal pathway', *Brain Stimulation*, 13: 931-938.
- Koch, Giacomo, Sonia Bonni, Maria Concetta Pellicciari, Elias P. Casula, Matteo Mancini, Romina Esposito, Viviana Ponzio, Silvia Picazio, Francesco Di Lorenzo, Laura Serra, Caterina Motta, Michele Maiella, Camillo Marra, Mara Cercignani, Alessandro Martorana, Carlo Caltagirone,

- and Marco Bozzali. 2018. 'Transcranial magnetic stimulation of the precuneus enhances memory and neural activity in prodromal Alzheimer's disease', *NeuroImage*, 169: 302-311.
- Koch, Giacomo, Michele Franca, Urs-Vito Albrecht, Carlo Caltagirone, and John C. Rothwell. 2006. 'Effects of paired pulse TMS of primary somatosensory cortex on perception of a peripheral electrical stimulus', *Experimental Brain Research*, 172: 416-424.
- Kolbinger, Hans Martin, Gereon Höflich, Andreas Hufnagel, Hans-Jürgen Müller, and Siegfried Kasper. 1995. 'Transcranial magnetic stimulation (TMS) in the treatment of major depression — a pilot study', *Human Psychopharmacology: Clinical and Experimental*, 10: 305-310.
- Koponen, Lari M., Jaakko O. Nieminen, and Risto J. Ilmoniemi. 2018. 'Multi-locus transcranial magnetic stimulation—theory and implementation', *Brain Stimulation*, 11: 849-855.
- Krings, T., H. Foltys, M. H. T. Reinges, S. Kemeny, V. Rohde, U. Spetzger, J. M. Gilsbach, and A. Thron. 2001. 'Navigated Transcranial Magnetic Stimulation for Presurgical Planning', *Minimally Invasive Neurosurgery*, 44: 234-239.
- Krings, Timo, Keith H. Chiappa, Henrik Foltys, Marcus H. Reinges, Rees G. Cosgrove, and Armin Thron. 2001. 'Introducing navigated transcranial magnetic stimulation as a refined brain mapping methodology', *Neurosurgical Review*, 24: 171-179.
- Laakso, Ilkka, and Akimasa Hirata. 2012. 'Fast multigrid-based computation of the induced electric field for transcranial magnetic stimulation', *Physics in Medicine and Biology*, 57: 7753-7765.
- Laakso, Ilkka, Marko Mikkonen, Soichiro Koyama, Akimasa Hirata, and Satoshi Tanaka. 2019. 'Can electric fields explain inter-individual variability in transcranial direct current stimulation of the motor cortex?', *Scientific Reports*, 9: 626.
- Laakso, Ilkka, Takenobu Murakami, Akimasa Hirata, and Yoshikazu Ugawa. 2018. 'Where and what TMS activates: Experiments and modeling', *Brain Stimulation*, 11: 166-174.
- Lancaster, Jack L., Shalini Narayana, Dennis Wenzel, James Luckemeyer, John Roby, and Peter Fox. 2004. 'Evaluation of an image-guided, robotically positioned transcranial magnetic stimulation system', *Human Brain Mapping*, 22: 329-240.
- Lebosse, C., P. Renaud, B. Bayle, and M. de Mathelin. 2011. 'Modeling and Evaluation of Low-Cost Force Sensors', *IEEE Transactions on Robotics*, 27: 815-822.
- Lebosse, C., P. Renaud, B. Bayle, M. de Mathelin, O. Piccin, and J. Foucher. 2007. "A robotic system for automated image-guided transcranial magnetic stimulation." In *2007 IEEE/NIH Life Science Systems and Applications Workshop*, 55-58.
- Lee, Hee-Don, Byeong-Kyu Lee, Wan-Soo Kim, Jung-Soo Han, Kyoo-Sik Shin, and Chang-Soo Han. 2014. 'Human-robot cooperation control based on a dynamic model of an upper limb exoskeleton for human power amplification', *Mechatronics*, 24: 168-176.
- Lee, W. H., S. H. Lisanby, A. F. Laine, and A. V. Peterchev. 2015. 'Electric Field Model of Transcranial Electric Stimulation in Nonhuman Primates: Correspondence to Individual Motor Threshold', *IEEE Transactions on Biomedical Engineering*, 62: 2095-2105.
- Lee, Wonhye, Stephanie D. Lee, Michael Y. Park, Lori Foley, Erin Purcell-Estabrook, Hyungmin Kim, Krisztina Fischer, Lee-So Maeng, and Seung-Schik Yoo. 2016. 'Image-Guided Focused Ultrasound-Mediated Regional Brain Stimulation in Sheep', *Ultrasound in Medicine and Biology*, 42: 459-470.
- Lefaucheur, J. P., P. Brugières, I. Ménard-Lefaucheur, S. Wendling, M. Pommier, and F. Bellivier. 2007. 'The value of navigation-guided rTMS for the treatment of depression: An illustrative case', *Neurophysiologie Clinique/Clinical Neurophysiology*, 37: 265-271.
- Leuze, C., G. Yang, B. Hargreaves, B. Daniel, and J. A. McNab. 2018. "Mixed-Reality Guidance for Brain Stimulation Treatment of Depression." In *2018 IEEE International Symposium on Mixed and Augmented Reality Adjunct (ISMAR-Adjunct)*, 377-380.
- Levkovitz, Yechiel, Moshe Isserles, Frank Padberg, Sarah H. Lisanby, Alexander Bystritsky, Guohua Xia, Aron Tendler, Zafiris J. Daskalakis, Jaron L. Winston, Pinhas Dannon, Hisham M. Hafez, Irving M. Reti, Oscar G. Morales, Thomas E. Schlaepfer, Eric Hollander, Joshua A. Berman, Mustafa M. Husain, Uzi Sofer, Ahava Stein, Shmulik Adler, Lisa Deutsch, Frederic Deutsch, Yiftach Roth, Mark S. George, and Abraham Zangen. 2015. 'Efficacy and safety of deep transcranial

- magnetic stimulation for major depression: a prospective multicenter randomized controlled trial', *World Psychiatry*, 14: 64-73.
- Li, Xingbao, Ziad Nahas, F. Andrew Kozel, Berry Anderson, Daryl E. Bohning, and Mark S. George. 2004. 'Acute left prefrontal transcranial magnetic stimulation in depressed patients is associated with immediately increased activity in prefrontal cortical as well as subcortical regions', *Biological Psychiatry*, 55: 882-890.
- Liere, R. van, and J. D. Mulder. 2003. "Optical tracking using projective invariant marker pattern properties." In *IEEE Virtual Reality, 2003. Proceedings.*, 191-198.
- Lin, Q., R. Yang, Z. Zhang, K. Cai, Z. Wang, M. Huang, J. Huang, Y. Zhan, and J. Zhuang. 2018. 'Robust Stereo-Match Algorithm for Infrared Markers in Image-Guided Optical Tracking System', *IEEE Access*, 6: 52421-52433.
- Lisanby, Sarah H., Mustafa M. Husain, Peter B. Rosenquist, Daniel Maixner, Rosben Gutierrez, Andrew Krystal, William Gilmer, Lauren B. Marangell, Scott Aaronson, Zafiris J. Daskalakis, Randolph Canterbury, Elliott Richelson, Harold A. Sackeim, and Mark S. George. 2008. 'Daily Left Prefrontal Repetitive Transcranial Magnetic Stimulation in the Acute Treatment of Major Depression: Clinical Predictors of Outcome in a Multisite, Randomized Controlled Clinical Trial', *Neuropsychopharmacology*, 34: 522.
- Lorenzen, H. W., and T. Weyh. 1992. 'Practical application of the summation method for 3-D static magnetic field calculation of a setup of conductive and ferromagnetic material', *IEEE Transactions on Magnetics*, 28: 1481-1484.
- Makarov, S. N., G. M. Noetscher, T. Raij, and A. Nummenmaa. 2018. 'A Quasi-Static Boundary Element Approach With Fast Multipole Acceleration for High-Resolution Bioelectromagnetic Models', *IEEE Transactions on Biomedical Engineering*, 65: 2675-2683.
- Makovac, Elena, Julian F. Thayer, and Cristina Ottaviani. 2017. 'A meta-analysis of non-invasive brain stimulation and autonomic functioning: Implications for brain-heart pathways to cardiovascular disease', *Neuroscience & Biobehavioral Reviews*, 74: 330-341.
- Mansouri, Farrokh, Arsalan Mir-Moghtadaei, Vanathy Niranjana, Jian Shu Wu, Daniyar Akhmedjanov, Mishael Nuh, Terri Cairo, Peter Giacobbe, José Zariffa, and Jonathan Downar. 2018. 'Development and validation of a 3D-printed neuronavigation headset for therapeutic brain stimulation', *Journal of Neural Engineering*, 15: 046034.
- Mascott, Christopher R., Jean-Christophe Sol, Philippe Bousquet, Jacques Lagarrigue, Yves Lazorthes, and Valérie Lauwers-Cances. 2006. 'Quantification of True In Vivo (Application) Accuracy in Cranial Image-guided Surgery: Influence of Mode of Patient Registration', *Operative Neurosurgery*, 59: ONS146-156.
- Mayberg, Helen S. 1997. 'Limbic-cortical dysregulation: a proposed model of depression', *The Journal of Neuropsychiatry and Clinical Neurosciences*, 9: 471-481.
- McConnell, Kathleen A., Ziad Nahas, Ananda Shastri, Jeffrey P. Lorberbaum, F. Andrew Kozel, Daryl E. Bohning, and Mark S. George. 2001. 'The transcranial magnetic stimulation motor threshold depends on the distance from coil to underlying cortex: a replication in healthy adults comparing two methods of assessing the distance to cortex', *Biological Psychiatry*, 49: 454-459.
- Meincke, Jonna, Manuel Hewitt, Giorgi Batsikadze, and David Liebetanz. 2016. 'Automated TMS hotspot-hunting using a closed loop threshold-based algorithm', *NeuroImage*, 124: 509-517.
- Meincke, Jonna, Manuel Hewitt, Markus Reischl, Rüdiger Rupp, Carsten Schmidt-Samoa, and David Liebetanz. 2018. 'Cortical representation of auricular muscles in humans: A robot-controlled TMS mapping and fMRI study', *PLoS ONE*, 13: e0201277.
- Michael, Jessica A., and Manreena Kaur. 2021. 'The Heart-Brain Connection in Depression: Can it inform a personalised approach for repetitive transcranial magnetic stimulation (rTMS) treatment?', *Neuroscience & Biobehavioral Reviews*, 127: 136-143.
- Mills, K. R., S. J. Boniface, and M. Schubert. 1992. 'Magnetic brain stimulation with a double coil: the importance of coil orientation', *Electroencephalography and Clinical Neurophysiology/Evoked Potentials Section*, 85: 17-21.

- Mir-Moghtadaei, Arsalan, Ruth Caballero, Peter Fried, Michael D. Fox, Katherine Lee, Peter Giacobbe, Zafiris J. Daskalakis, Daniel M. Blumberger, and Jonathan Downar. 2015. 'Concordance Between BeamF3 and MRI-neuronavigated Target Sites for Repetitive Transcranial Magnetic Stimulation of the Left Dorsolateral Prefrontal Cortex', *Brain Stimulation*, 8: 965-973.
- Mir-Moghtadaei, Arsalan, Peter Giacobbe, Zafiris J. Daskalakis, Daniel M. Blumberger, and Jonathan Downar. 2016. 'Validation of a 25% Nasion–Inion Heuristic for Locating the Dorsomedial Prefrontal Cortex for Repetitive Transcranial Magnetic Stimulation', *Brain Stimulation*, 9: 793-795.
- Miranda, P. C., M. Hallett, and P. J. Basser. 2003. 'The electric field induced in the brain by magnetic stimulation: a 3-D finite-element analysis of the effect of tissue heterogeneity and anisotropy', *IEEE Transactions on Biomedical Engineering*, 50: 1074-1085.
- Moisa, Marius, Rolf Pohmann, Lars Ewald, and Axel Thielscher. 2009. 'New coil positioning method for interleaved transcranial magnetic stimulation (TMS)/functional MRI (fMRI) and its validation in a motor cortex study', *Journal of Magnetic Resonance Imaging*, 29: 189-197.
- Momi, Davide, Recep A. Ozdemir, Ehsan Tadayon, Pierre Boucher, Mouhsin M. Shafi, Alvaro Pascual-Leone, and Emiliano Santarnecchi. 2021. 'Network-level macroscale structural connectivity predicts propagation of transcranial magnetic stimulation', *NeuroImage*, 229: 117698.
- Mylius, V., S. S. Ayache, R. Ahdab, W. H. Farhat, H. G. Zouari, M. Belke, P. Brugières, E. Wehrmann, K. Krakow, N. Timmesfeld, S. Schmidt, W. H. Oertel, S. Knake, and J. P. Lefaucheur. 2013. 'Definition of DLPFC and M1 according to anatomical landmarks for navigated brain stimulation: Inter-rater reliability, accuracy, and influence of gender and age', *NeuroImage*, 78: 224-232.
- Neggers, S. F. W., T. R. Langerak, D. J. L. G. Schutter, R. C. W. Mandl, N. F. Ramsey, P. J. J. Lemmens, and A. Postma. 2004. 'A stereotactic method for image-guided transcranial magnetic stimulation validated with fMRI and motor-evoked potentials', *NeuroImage*, 21: 1805-1817.
- Noirhomme, Q., M. Ferrant, Y. Vandermeeren, E. Olivier, B. Macq, and O. Cuisenaire. 2004. 'Registration and real-time visualization of transcranial magnetic stimulation with 3-D MR images', *IEEE Transactions on Biomedical Engineering*, 51: 1994-2005.
- Nummenmaa, Aapo, Jennifer A. McNab, Peter Savadjiev, Yoshio Okada, Matti S. Hämäläinen, Ruopeng Wang, Lawrence L. Wald, Alvaro Pascual-Leone, Van J. Wedeen, and Tommi Raij. 2014. 'Targeting of White Matter Tracts with Transcranial Magnetic Stimulation', *Brain Stimulation*, 7: 80-84.
- Oliver, R., O. Bjoertomt, J. Driver, R. Greenwood, and J. Rothwell. 2009. 'Novel 'hunting' method using transcranial magnetic stimulation over parietal cortex disrupts visuospatial sensitivity in relation to motor thresholds', *Neuropsychologia*, 47: 3152-3161.
- Opitz, Alexander, Wynn Legon, Abby Rowlands, Warren K. Bickel, Walter Paulus, and William J. Tyler. 2013. 'Physiological observations validate finite element models for estimating subject-specific electric field distributions induced by transcranial magnetic stimulation of the human motor cortex', *NeuroImage*, 81: 253-264.
- Opitz, Alexander, Mirko Windhoff, Robin M. Heidemann, Robert Turner, and Axel Thielscher. 2011. 'How the brain tissue shapes the electric field induced by transcranial magnetic stimulation', *NeuroImage*, 58: 849-859.
- Paffi, Alessandra, Francesca Camera, Filippo Carducci, Gianluigi Rubino, Paolo Tampieri, Micaela Liberti, and Francesca Apollonio. 2015. 'A Computational Model for Real-Time Calculation of Electric Field due to Transcranial Magnetic Stimulation in Clinics.', *International Journal of Antennas and Propagation*: 976854.
- Paillère Martinot, Marie-Laure, André Galinowski, Damien Ringuenet, Thierry Gallarda, Jean-Pascal Lefaucheur, Frank Bellivier, Christine Picq, Pascale Bruguière, Jean-François Mangin, Denis Rivière, Jean-Claude Willer, Bruno Falissard, Marion Leboyer, Jean-Pierre Olié, Eric Artiges, and Jean-Luc Martinot. 2010. 'Influence of prefrontal target region on the efficacy of repetitive transcranial magnetic stimulation in patients with medication-resistant depression: a [18F]-fluorodeoxyglucose PET and MRI study', *International Journal of Neuropsychopharmacology*, 13: 45-59.

- Pascual-Leone, Alvaro, Belen Rubio, Federico Pallardó, and Maria Dolores Catalá. 1996. 'Rapid-rate transcranial magnetic stimulation of left dorsolateral prefrontal cortex in drug-resistant depression', *The Lancet*, 348: 233-237.
- Pascual-Leone, Alvaro, John R. Gates, and Anil Dhuna. 1991. 'Induction of speech arrest and counting errors with rapid-rate transcranial magnetic stimulation', *Neurology*, 41: 697-702.
- Paus, Tomas. 1998. 'Imaging the brain before, during, and after transcranial magnetic stimulation', *Neuropsychologia*, 37: 219-224.
- Paus, Tomáš, Robert Jech, Christopher J. Thompson, Roch Comeau, Terry Peters, and Alan C. Evans. 1997. 'Transcranial Magnetic Stimulation during Positron Emission Tomography: A New Method for Studying Connectivity of the Human Cerebral Cortex', *The Journal of Neuroscience*, 17: 3178-3184.
- Pfisterer, Wolfgang K., Stephen Papadopoulos, Denise A. Drumm, Kris Smith, and Mark C. Preul. 2008. 'Fiducial Versus Nonfiducial Neuronavigation Registration Assessment and Considerations of Accuracy', *Operative Neurosurgery*, 62: ONS201-208.
- Picht, Thomas, Sven Mularski, Bjoern Kuehn, Peter Vajkoczy, Theodoros Kombos, and Olaf Suess. 2009. 'Navigated Transcranial Magnetic Stimulation for Preoperative Functional Diagnostics in Brain Tumor Surgery', *Operative Neurosurgery*, 65: ONS93-99.
- Picht, Thomas, Sein Schmidt, Stephan Brandt, Dietmar Frey, Henri Hannula, Tuomas Neuvonen, Jari Karhu, Peter Vajkoczy, and Olaf Suess. 2011. 'Preoperative Functional Mapping for Rolandic Brain Tumor Surgery: Comparison of Navigated Transcranial Magnetic Stimulation to Direct Cortical Stimulation', *Neurosurgery*, 69: 581-589.
- Pinton, Gianmarco, Jean-Francois Aubry, Emmanuel Bossy, Marie Muller, Mathieu Pernot, and Mickael Tanter. 2012. 'Attenuation, scattering, and absorption of ultrasound in the skull bone', *Medical Physics*, 39: 299-307.
- Pletinckx, Daniel. 1989. 'Quaternion calculus as a basic tool in computer graphics', *The Visual Computer*, 5: 2-13.
- Pommier, Benjamin, François Vassal, Claire Boutet, Sophie Jeannin, Roland Peyron, and Isabelle Faillenot. 2017. 'Easy methods to make the neuronavigated targeting of DLPFC accurate and routinely accessible for rTMS', *Neurophysiologie Clinique/Clinical Neurophysiology*, 47: 35-46.
- Poulin, François, and L. P. Amiot. 2002. 'Interference during the use of an electromagnetic tracking system under OR conditions', *Journal of Biomechanics*, 35: 733-737.
- Pulopulos, Matias M., Maximilian Schmausser, Stefanie De Smet, Marie-Anne Vanderhasselt, Shishir Baliyan, César Venero, Chris Baeken, and Rudi De Raedt. 2020. 'The effect of HF-rTMS over the left DLPFC on stress regulation as measured by cortisol and heart rate variability', *Hormones and Behavior*, 124: 104803.
- Raffin, Estelle, Giovanni Pellegrino, Vincenzo Di Lazzaro, Axel Thielscher, and Hartwig Roman Siebner. 2015. 'Bringing transcranial mapping into shape: Sulcus-aligned mapping captures motor somatotopy in human primary motor hand area', *NeuroImage*, 120: 164-175.
- Raij, Tommi, Apo Nummenmaa, Marie-France Marin, Daria Porter, Sharon Furtak, Kawin Setsompop, and Mohammed R. Milad. 2018. 'Prefrontal Cortex Stimulation Enhances Fear Extinction Memory in Humans', *Biological Psychiatry*, 84: 129-137.
- Rajput, O., N. Gessert, M. Gromniak, L. Matthäus, and A. Schlaefer. 2018. 'Towards head motion compensation using multi-scale convolutional neural networks', *arXiv*, 1807.03651.
- Rawji, Vishal, Matteo Ciocca, André Zacharia, David Soares, Dennis Truong, Marom Bikson, John Rothwell, and Sven Bestmann. 2018. 'tDCS changes in motor excitability are specific to orientation of current flow', *Brain Stimulation*, 11: 289-298.
- Richter, L. 2013. *Robotized transcranial magnetic stimulation* (Springer: New York).
- Richter, L., R. Bruder, A. Schlaefer, and A. Schweikard. 2010. "Towards direct head navigation for robot-guided Transcranial Magnetic Stimulation using 3D laserscans: Idea, setup and feasibility." In *IEEE Proc. Engin. Med. Biol*, 2283-2286.
- Richter, L., L. Matthäus, A. Schlaefer, and A. Schweikard. 2010. "Fast robotic compensation of spontaneous head motion during Transcranial Magnetic Stimulation (TMS)." In *IET UKACC International Conference on Control 2010*, 1-6.

- Richter, Lars, and Ralf Bruder. 2013. 'Design, implementation and evaluation of an independent real-time safety layer for medical robotic systems using a force–torque–acceleration (FTA) sensor', *International Journal of Computer Assisted Radiology and Surgery*, 8: 429-436.
- Richter, Lars, Ralf Bruder, and Achim Schweikard. 2012. 'Hand-assisted positioning and contact pressure control for motion compensated robotized transcranial magnetic stimulation', *International Journal of Computer Assisted Radiology and Surgery*, 7: 845-852.
- Richter, Lars, Gunnar Neumann, Stephen Oung, Achim Schweikard, and Peter Trillenber. 2013. 'Optimal Coil Orientation for Transcranial Magnetic Stimulation', *PLoS ONE*, 8: e60358.
- Richter, Lars, Peter Trillenber, Achim Schweikard, and Alexander Schlaefer. 2013. 'Stimulus Intensity for Hand Held and Robotic Transcranial Magnetic Stimulation', *Brain Stimulation*, 6: 315-321.
- Rizzo, Vincenzo, Hartwig R. Siebner, Nicola Modugno, Alessandra Pesenti, Alexander Münchau, Willibald Gerschlag, Ruth M. Webb, and John C. Rothwell. 2004. 'Shaping the excitability of human motor cortex with premotor rTMS', *The Journal of Physiology*, 554: 483-495.
- Ro, Tony, Alessandro Farnè, and Erik Chang. 2002. 'Locating the Human Frontal Eye Fields With Transcranial Magnetic Stimulation', *Journal of Clinical and Experimental Neuropsychology*, 24: 930-940.
- Rodseth, Jakob, Edward P. Washabaugh, and Chandramouli Krishnan. 2017. 'A novel low-cost approach for navigated transcranial magnetic stimulation', *Restorative Neurology and Neuroscience*, 35: 601-609.
- Ruohonen, J., and R. J. Ilmoniemi. 1998. 'Focusing and targeting of magnetic brain stimulation using multiple coils', *Medical and Biological Engineering and Computing*, 36: 297-301.
- Sack, Alexander T., Roi Cohen Kadosh, Teresa Schuhmann, Michelle Moerel, Vincent Walsh, and Rainer Goebel. 2009. 'Optimizing Functional Accuracy of TMS in Cognitive Studies: A Comparison of Methods', *Journal of Cognitive Neuroscience*, 21: 207-221.
- Salminen-Vaparanta, Niina, Simo Vanni, Valdas Noreika, Vidas Valiulis, Levente Móró, and Antti Revonsuo. 2014. 'Subjective Characteristics of TMS-Induced Phosphenes Originating in Human V1 and V2', *Cerebral Cortex*, 24: 2751-2760.
- Sathyanarayana, Supriya, Christoph Leuze, Brian Hargreaves, Bruce Daniel, Gordon Wetzstein, Amit Etkin, Mahendra Bhati, and Jennifer McNab. 2020. "Comparison of head pose tracking methods for mixed-reality neuronavigation for transcranial magnetic stimulation", In *Medical Imaging 2020, Image-Guided Procedures, Robotic Interventions, and Modeling (SPIE)*, 11315: 113150L.
- Saturnino, Guilherme B., André Antunes, and Axel Thielscher. 2015. 'On the importance of electrode parameters for shaping electric field patterns generated by tDCS', *NeuroImage*, 120: 25-35.
- Schmidt, Sein, Rouven Bathe-Peters, Robert Fleischmann, Maria Rönnefarth, Michael Scholz, and Stephan A. Brandt. 2015. 'Nonphysiological factors in navigated TMS studies; Confounding covariates and valid intracortical estimates', *Human Brain Mapping*, 36: 40-49.
- Schönfeldt-Lecuona, C., J. P. Lefaucheur, L. Cardenas-Morales, R. C. Wolf, T. Kammer, and U. Herwig. 2010. 'The value of neuronavigated rTMS for the treatment of depression', *Neurophysiologie Clinique/Clinical Neurophysiology*, 40: 37-43.
- Schönfeldt-Lecuona, Carlos, Axel Thielscher, Roland W. Freudenmann, Martina Kron, Manfred Spitzer, and Uwe Herwig. 2005. 'Accuracy of Stereotaxic Positioning of Transcranial Magnetic Stimulation', *Brain Topography*, 17: 253-259.
- Schubert, M., A. Curt, L. Jensen, and V. Dietz. 1997. 'Corticospinal input in human gait: modulation of magnetically evoked motor responses', *Experimental Brain Research*, 115: 234-246.
- Seibt, Ole, Andre R. Brunoni, Yu Huang, and Marom Bikson. 2015. 'The Pursuit of DLPFC: Non-neuronavigated Methods to Target the Left Dorsolateral Pre-frontal Cortex With Symmetric Bicephalic Transcranial Direct Current Stimulation (tDCS)', *Brain Stimulation*, 8: 590-602.
- Seyal, Masud, Lorainne K. Masuoka, and John K. Browne. 1992. 'Suppression of cutaneous perception by magnetic pulse stimulation of the human brain', *Electroencephalography and Clinical Neurophysiology/Evoked Potentials Section*, 85: 397-401.

- Shiakolas, P. S., K. L. Conrad, and T. C. Yih. 2002. 'On the Accuracy, Repeatability, and Degree of Influence of Kinematics Parameters for Industrial Robots', *International Journal of Modelling and Simulation*, 22: 245-254.
- Sollmann, Nico, Noriko Tanigawa, Lucia Bulubas, Jamil Sabih, Claus Zimmer, Florian Ringel, Bernhard Meyer, and Sandro M. Krieg. 2017. 'Clinical Factors Underlying the Inter-individual Variability of the Resting Motor Threshold in Navigated Transcranial Magnetic Stimulation Motor Mapping', *Brain Topography*, 30: 98-121.
- Sommer, Martin, Matteo Ciocca, Raffaella Chieffo, Paul Hammond, Andreas Neef, Walter Paulus, John C. Rothwell, and Ricci Hannah. 2018. 'TMS of primary motor cortex with a biphasic pulse activates two independent sets of excitable neurones', *Brain Stimulation*, 11: 558-565.
- Sorriento, A., M. B. Porfido, S. Mazzoleni, G. Calvosa, M. Tenucci, G. Ciuti, and P. Dario. 2020. 'Optical and Electromagnetic Tracking Systems for Biomedical Applications: A Critical Review on Potentialities and Limitations', *IEEE Reviews in Biomedical Engineering*, 13: 212-232.
- Soteriou, Eric, Juergen Grauvogel, Roland Laszig, and Tanja Daniela Grauvogel. 2016. 'Prospects and limitations of different registration modalities in electromagnetic ENT navigation', *European Archives of Oto-Rhino-Laryngology*, 273: 3979-3986.
- Souza, Victor Hugo, Renan H. Matsuda, André S. C. Peres, Paulo Henrique J. Amorim, Thiago F. Moraes, Jorge Vicente L. Silva, and Oswaldo Baffa. 2018. 'Development and characterization of the InVesalius Navigator software for navigated transcranial magnetic stimulation', *Journal of Neuroscience Methods*, 309: 109-120.
- Sparing, Roland, Dorothee Buelte, Ingo G. Meister, Tomás Pauš, and Gereon R. Fink. 2008. 'Transcranial magnetic stimulation and the challenge of coil placement: A comparison of conventional and stereotaxic neuronavigational strategies', *Human Brain Mapping*, 29: 82-96.
- Stahl, J. S. 1999. 'Amplitude of human head movements associated with horizontal saccades', *Experimental Brain Research*, 126: 41-54.
- States, R. A., and E. Pappas. 2006. 'Precision and repeatability of the Optotrak 3020 motion measurement system', *Journal of Medical Engineering & Technology*, 30: 11-16.
- Stenroos, Matti, and Lari M Koponen. 2019. 'Real-time computation of the TMS-induced electric field in a realistic head model', *bioRxiv*: 547315.
- Stieglitz, Lennart Henning, Jens Fichtner, Robert Andres, Philippe Schucht, Ann-Kathrin Krähenbühl, Andreas Raabe, and Jürgen Beck. 2013. 'The Silent Loss of Neuronavigation Accuracy: A Systematic Retrospective Analysis of Factors Influencing the Mismatch of Frameless Stereotactic Systems in Cranial Neurosurgery', *Neurosurgery*, 72: 796-807.
- Stokes, Mark G., Christopher D. Chambers, Ian C. Gould, Tracy R. Henderson, Natasha E. Janko, Nicholas B. Allen, and Jason B. Mattingley. 2005. 'Simple Metric For Scaling Motor Threshold Based on Scalp-Cortex Distance: Application to Studies Using Transcranial Magnetic Stimulation', *Journal of Neurophysiology*, 94: 4520-4527.
- Takahashi, Satoshi, and Thomas Picht. 2014. 'Comparison of Navigated Transcranial Magnetic Stimulation to Direct Electrical Stimulation for Mapping the Motor Cortex Prior to Brain Tumor Resection.' in M. A. Hayat (ed.), *Tumors of the Central Nervous System, Volume 12: Molecular Mechanisms, Children's Cancer, Treatments, and Radiosurgery* (Springer Netherlands: Dordrecht).
- Tambini, Arielle, Derek Evan Nee, and Mark D'Esposito. 2018. 'Hippocampal-targeted Theta-burst Stimulation Enhances Associative Memory Formation', *Journal of Cognitive Neuroscience*, 30: 1452-1472.
- Tao, Qi, Yongfeng Yang, Hongyan Yu, Lingzhong Fan, Shuxin Luan, Lei Zhang, Hua Zhao, Luxian Lv, Tianzi Jiang, and Xueqin Song. 2020. 'Anatomical Connectivity-Based Strategy for Targeting Transcranial Magnetic Stimulation as Antidepressant Therapy', *Frontiers in Psychiatry*, 11: 236.
- Taube, Wolfgang, Christian Leukel, Martin Schubert, Markus Gruber, Timo Rantalainen, and Albert Gollhofer. 2008. 'Differential Modulation of Spinal and Corticospinal Excitability During Drop Jumps', *Journal of Neurophysiology*, 99: 1243-1252.

- Teitti, S., S. Määttä, L. Säisänen, M. Könönen, R. Vanninen, H. Hannula, E. Mervaala, and J. Karhu. 2008. 'Non-primary motor areas in the human frontal lobe are connected directly to hand muscles', *NeuroImage*, 40: 1243-1250.
- Thielscher, Axel, and Thomas Kammer. 2002. 'Linking Physics with Physiology in TMS: A Sphere Field Model to Determine the Cortical Stimulation Site in TMS', *NeuroImage*, 17: 1117-1130.
- . 2004. 'Electric field properties of two commercial figure-8 coils in TMS: calculation of focality and efficiency', *Clinical Neurophysiology*, 115: 1697-1708.
- Thielscher, Axel, Alexander Opitz, and Mirko Windhoff. 2011. 'Impact of the gyral geometry on the electric field induced by transcranial magnetic stimulation', *NeuroImage*, 54: 234-243.
- Topp, Eric L., and Carolyn Patten. 2015. 'Securing a TMS coil to the patients head', University of Florida Research Foundation, Patent US 9,724,532, US 2015/0202453, U.S. Patent and Trademark Office.
- Traad, M. 1990. 'A Quantitative Positioning Device For Transcranial Magnetic Stimulation', *Proc. IEEE Eng. Med. Biol. Soc. (EMBC)*, 12: 2246-2246.
- Trapp, Nicholas T., Joel Bruss, Marcie King Johnson, Brandt D. Uitermarkt, Laren Garrett, Amanda Heinzerling, Chaorong Wu, Timothy R. Kosciak, Patrick Ten Eyck, and Aaron D. Boes. 2020. 'Reliability of targeting methods in TMS for depression: Beam F3 vs. 5.5 cm', *Brain Stimulation*, 13: 578-581.
- Treleaven, Julia. 2008. 'Sensorimotor disturbances in neck disorders affecting postural stability, head and eye movement control', *Manual Therapy*, 13: 2-11.
- Tufail, Yusuf, Alexei Matyushov, Nathan Baldwin, Monica L. Tauchmann, Joseph Georges, Anna Yoshihiro, Stephen I. Helms Tillery, and William J. Tyler. 2010. 'Transcranial Pulsed Ultrasound Stimulates Intact Brain Circuits', *Neuron*, 66: 681-694.
- Tufail, Yusuf, Anna Yoshihiro, Sandipan Pati, Monica M. Li, and William J. Tyler. 2011. 'Ultrasonic neuromodulation by brain stimulation with transcranial ultrasound', *Nature Protocols*, 6: 1453.
- Ulrich, Martin, Sabrina Lorenz, Markus W. Spitzer, Leon Steigleder, Thomas Kammer, and Georg Grön. 2018. 'Theta-burst modulation of mid-ventrolateral prefrontal cortex affects salience coding in the human ventral tegmental area', *Appetite*, 123: 91-100.
- Van Essen, David C., Heather A. Drury, Sarang Joshi, and Michael I. Miller. 1998. 'Functional and structural mapping of human cerebral cortex: Solutions are in the surfaces', *Proceedings of the National Academy of Sciences*, 95: 788-795.
- Villamar, Mauricio F., Magdalena Sarah Volz, Marom Bikson, Abhishek Datta, Alexandre F. DaSilva, and Felipe Fregni. 2013. 'Technique and Considerations in the Use of 4x1 Ring High-definition Transcranial Direct Current Stimulation (HD-tDCS)', *Journal of Visualized Experiments (JoVE)*: 50309.
- Volz, Lukas J., Masashi Hamada, John C. Rothwell, and Christian Grefkes. 2015. 'What Makes the Muscle Twitch: Motor System Connectivity and TMS-Induced Activity', *Cerebral Cortex*, 25: 2346-2353.
- Walsh, Vincent, Amanda Ellison, Lorella Battelli, and Alan Cowey. 1998. 'Task-specific impairments and enhancements induced by magnetic stimulation of human visual area V5', *Proceedings of the Royal Society of London. Series B: Biological Sciences*, 265: 537-543.
- Wang, Jane X., Lynn M. Rogers, Evan Z. Gross, Anthony J. Ryals, Mehmet E. Dokucu, Kelly L. Brandstatt, Molly S. Hermiller, and Joel L. Voss. 2014. 'Targeted enhancement of cortical-hippocampal brain networks and associative memory', *Science*, 345: 1054-1057.
- Wang, Man Ning, and Zhi Jian Song. 2011. 'Classification and Analysis of the Errors in Neuronavigation', *Neurosurgery*, 68: 1131-1143.
- Washabaugh, Edward P., and Chandramouli Krishnan. 2016. 'A low-cost system for coil tracking during transcranial magnetic stimulation', *Restorative Neurology and Neuroscience*, 34: 337-346.
- Wassermann, Eric M., Binseng Wang, Thomas A. Zeffiro, Norihiro Sadato, Alvaro Pascual-Leone, Camilo Toro, and Mark Hallett. 1996. 'Locating the Motor Cortex on the MRI with Transcranial Magnetic Stimulation and PET', *NeuroImage*, 3: 1-9.

- Wattiez, Nicolas, Charlotte Constans, Thomas Deffieux, Pierre M. Daye, Mickael Tanter, Jean-François Aubry, and Pierre Pouget. 2017. 'Transcranial ultrasonic stimulation modulates single-neuron discharge in macaques performing an antisaccade task', *Brain Stimulation*, 10: 1024-1031.
- Weiduschat, Nora, Birgit Habedank, Birgit Lampe, Jörg Poggenborg, Alexander Schuster, Walter F. Haupt, Wolf Dieter Heiss, and Alexander Thiel. 2009. 'Localizing Broca's area for transcranial magnetic stimulation: Comparison of surface distance measurements and stereotaxic positioning', *Brain Stimulation*, 2: 93-102.
- Weigand, Anne, Andreas Horn, Ruth Caballero, Danielle Cooke, Adam P. Stern, Stephan F. Taylor, Daniel Press, Alvaro Pascual-Leone, and Michael D. Fox. 2018. 'Prospective Validation That Subgenual Connectivity Predicts Antidepressant Efficacy of Transcranial Magnetic Stimulation Sites', *Biological Psychiatry*, 84: 28-37.
- Weise, Konstantin, Ole Numssen, Axel Thielscher, Gesa Hartwigsen, and Thomas R. Knösche. 2020. 'A novel approach to localize cortical TMS effects', *NeuroImage*, 209: 116486.
- Weiss Lucas, Carolin, Charlotte Nettekoven, Volker Neuschmelting, Ana-Maria Oros-Peusquens, Gabriele Stoffels, Shivakumar Viswanathan, Anne K. Rehme, Andrea Maria Faymonville, N. Jon Shah, Karl Josef Langen, Roland Goldbrunner, and Christian Grefkes. 2020. 'Invasive versus non-invasive mapping of the motor cortex', *Human Brain Mapping*, 41: 3970-3983.
- Westin, Gregory G., Bruce D. Bassi, Sarah H. Lisanby, and Bruce Luber. 2014. 'Determination of motor threshold using visual observation overestimates transcranial magnetic stimulation dosage: Safety implications', *Clinical Neurophysiology*, 125: 142-147.
- Wiles, Andrew, David Thompson, and Donald Frantz. 2004. "Accuracy assessment and interpretation for optical tracking systems", In *Medical Imaging 2004, Visualization, Image-Guided Procedures, and Display (SPIE)*, 5367: 421-432.
- Wilson, S. A., G. W. Thickbroom, and F. L. Mastaglia. 1993. 'Transcranial magnetic stimulation mapping of the motor cortex in normal subjects: The representation of two intrinsic hand muscles', *Journal of the Neurological Sciences*, 118: 134-144.
- Woerdeman, Peter A., Peter W. A. Willems, Herke J. Noordmans, Cornelis A. F. Tulleken, and Jan Willem Berkelbach van der Sprenkel. 2007. 'Application accuracy in frameless image-guided neurosurgery: a comparison study of three patient-to-image registration methods', *Journal of Neurosurgery JNS*, 106: 1012-1016.
- Wölfel, Markus, Christian Hirschbeck, and Kerstin Häringer. 2018. 'Positioning aid for TMS', Mag & More GmbH, Patent EP 3 372 278, European Patent Office.
- Woods, A. J., A. Antal, M. Bikson, P. S. Boggio, A. R. Brunoni, P. Celnik, L. G. Cohen, F. Fregni, C. S. Herrmann, E. S. Kappenman, H. Knotkova, D. Liebetanz, C. Miniussi, P. C. Miranda, W. Paulus, A. Priori, D. Reato, C. Stagg, N. Wenderoth, and M. A. Nitsche. 2016. 'A technical guide to tDCS, and related non-invasive brain stimulation tools', *Clinical Neurophysiology*, 127: 1031-1048.
- Woods, Adam J., Vaughn Bryant, Daniela Sacchetti, Felix Gervits, and Roy Hamilton. 2015. 'Effects of Electrode Drift in Transcranial Direct Current Stimulation', *Brain Stimulation*, 8: 515-519.
- Wu, Han, Qinyong Lin, Rongqian Yang, Yuan Zhou, Lingxiang Zheng, Yueshan Huang, Zhigang Wang, Yonghua Lao, and Jinhua Huang. 2019. 'An Accurate Recognition of Infrared Retro-Reflective Markers in Surgical Navigation', *Journal of Medical Systems*, 43: 153.
- Xiao, Z., Q. Ruan, and X. Wang. 2018. "CortexBot: 3D Visual Fusion of Robotic Neuronavigated TMS System." In *2018 IEEE International Conference on Cyborg and Bionic Systems (CBS)*, 406-411.
- Yan, Guanghua, Jonathan Li, Yin Huang, Kathryn Mittauer, Bo Lu, and Chihray Liu. 2014. 'Ghost marker detection and elimination in marker-based optical tracking systems for real-time tracking in stereotactic body radiotherapy', *Medical Physics*, 41: 101713.
- Yuen, H. K., J. Princen, J. Illingworth, and J. Kittler. 1990. 'Comparative study of Hough Transform methods for circle finding', *Image and Vision Computing*, 8: 71-77.
- Zhang, Q., X. Wang, and Z. Lin. 2018. "A New Head Location Method in TMS Treatment." In *2018 IEEE International Conference on Information and Automation (ICIA)*, 1398-1403.

- Zhou, Zhentian, Bo Wu, Juan Duan, Xu Zhang, Nan Zhang, and Zhiyuan Liang. 2017. 'Optical surgical instrument tracking system based on the principle of stereo vision', *Journal of Biomedical Optics*, 22: 1-14.
- Zorn, L., P. Renaud, B. Bayle, L. Goffin, C. Lebosse, M. de Mathelin, and J. Foucher. 2012. 'Design and Evaluation of a Robotic System for Transcranial Magnetic Stimulation', *IEEE Transactions on Biomedical Engineering*, 59: 805-815.